2023-07

Flood Inundation mapping Using HEC-RAS and Geospatial Techniques: The Case of Suha River, Blue Nile Basin, Ethiopia

Birhane, Seifu

BAHIRDAR UNIVERRSITY

BAHIRDAR INSTITUTE OF TECHNOLOGY

SCHOOL OF GRADUATE STUDIES

FACULTY OF CIVIL AND WATER RESOURCES ENGINEERING

Flood Inundation mapping Using HEC-RAS and Geospatial Techniques: The Case of Suha River, Blue Nile Basin, Ethiopia

By

Birhane Seifu

July, 2023

BAHIR DAR, ETHIOPIA

FLOOD INUNDATION MAPPING USING HEC-RAS AND GEOSPATIAL TECHNIQUES: THE CASE OF SUHA RIVER, BLUE NILE BASIN, ETHIOPIA

BIRHANE SEIFU

A thesis submitted to School of Graduate Studies of Bahir Dar Institute of Technology, Bahir Dar University In Partial Fulfillment of the Requirements for the Degree of Master of Science in Hydraulics in Faculty of Civil and Water Resources Engineering.

ADVISOR: EPHREM YETBAREK (PhD)

July, 2023

BAHIR DAR, ETHIOPIA

DECLARATION

This is to certify that the thesis entitled " **Flood Inundation mapping Using HEC-RAS and Geospatial Techniques: The Case of Suha River, Blue Nil Basin, Ethiopia"**, submitted in partial fulfillment of the requirements for the degree of Master of Science in Hydraulic Engineering under the faculty of Civil and Water Resources Engineering, Bahir Dar Institute of Technology, is a record of original work carried out by me and has never been submitted to this or any other institution to get any other degree or certificates. The assistance and help I received during the course of this investigation have been duly acknowledged.

Birhane Seifu		21/07/2023
Name of student	Signature	Date

BAHIR DAR UNIVERSITY
BAHIR DAR INSTITUTE OF TECHNOLOGY

SCHOOL OF GRADUATE STUDIES
FACULTY OF CIVIL AND WATER RESOURCE ENGINEERING

APPROVAL SHEET

Name of Student Ephrem Sch Signature _____ Date 20-7-2023

The following graduate faculty members certify that this student has successfully presented the necessary written thesis and oral presentation of this thesis for partial fulfillment of the thesis option requirements for the degree of master's sciences in hydraulic engineering.

Board of Examiners

Name of Advisor	Signature	Date
Eshetie Yehuala, PhD		20-7-2023
Name of External examiner	Signature	Date
Adugnaw Tadesse (PhD)		July 19, 2023
Name of Internal Examiner	Signature	Date
Mengiste Abate (PhD)		JULY 20 2023
Name of Chairperson	Signature	Date
Habtamu Debalqe		July 20 2023
Name of Chair Holder	Signature	Date
Mengistu Abate (PhD)		20/7/2023
Name of Faculty Dean Melkamu Demewez Gebeye Faculty Academic Program Officer (V/Dean)	Signature	Date JULY 20/2023

Faculty Stamp

ACKNOWLEDGEMET

First, I would like to thank the Almighty GOD, his mother, Saint Marry and, all his Angels and Saints for their blessing and grace upon me during my works and in all my life. GOD, not only do you give a lot through my life but also keep my mental strength in my education.

I would like to express sincere gratitude to my thesis advisor, Ephrem Yetbarek (PhD), for his valuable guidance and encouragement, starting from the selection of the problem solver title up to this final thesis work. I would also like to thank my examiners, both during the proposal and progress presentation, for their valuable time to review my work and give supportive suggestions that have helped me to reach this final thesis.

Last but not least, I would like to thank all my family members and friends for their love, care, and prayers for me throughout my life.

ABSTRACT

Flood is the devastating natural events as it causes massive destructive of life, economy and infrastructure. The main objective of this study was Flood Inundation mapping Using HEC-RAS and Geospatial Techniques. Different models, including the hydraulic model (HEC-RAS) and the hydrological model (HEC-HMS) integrating ArcGIS were used for conducting this study. Primary data such as river cross sections, and secondary data such as rainfall, stream flow, digital elevation model (DEM), land use, land cover, and soil type were collected and used for the study. Totally, around 19 years of observed flow data 13 years (1986–1998) for calibration and 6 years (1999–2004) for validation were used. It is observed that HEC-HMS calibration and validation results were good, and the performance of the model was checked with the Nash Sutcliffe Efficiency, root mean square error, and percent of bias. Values of 0.723, 0.57, and 10.83 for calibration and 0.753, 0.485, and 8.253 for validation were obtained for NSE, RMSE, and PBIAS, respectively. The peak flood magnitude obtained for 2, 5, 10, 25, 50, and 100 years return periods were 50.4, 76.1, 107, 151.9, 211, and 301 m^3/s, respectively. The HEC-RAS model calibration and validation results were compared using satellite images downloaded from Landsat 7 and a relatively good result was obtained. The flood inundation map is prepared using the RAS Mapper tool and different flood inundation maps are obtained for different return periods. The flood inundation map covers 100.8, 151.5, 200, 280, 350.2, and 453 ha for 2, 5, 10, 25, 50, and 100 year return periods, respectively. Therefore, in order to mitigate these damages, both structural and nonstructural measures are recommended, depending on the severity of the damage at each station.

Key words: flood inundation mapping, HEC-RAS, Suha River, RAS Mapper, HEC-HMS

CONTENTS PAGES

LIST OF TABLES

LIST OF FIGURES

LIST OF ABBREVIATION

ARC-GIS	Aeronautical Reconnaissance coverage geographic information system
CN	Curve number
DEM	Digital elevation model
ERA	Ethiopian road authority
GPS	Global positioning system
HEC-HMS	Hydrologic engineering center for Hydrologic modeling system
HEC-RAS	Hydrologic engineering center for river analysis system
HEC-FDA	Hydrologic engineering center for flood damage reduction analysis
HSG	Hydrologic soil group
LULC	Land use land cover
MoWIE	Ministry of water, irrigation and energy
NMA	National meteorological Agency
RP	Return period
SCS	Soil conservation service

1. INTRODUCTION

1.1 Background

Rivers and river systems are very important to human beings. As history has shown us, most civilizations are built around rivers (Getahun et al., 2015). Even though rivers and their adjacent floodplain corridors fulfill a variety of functions both as part of the natural ecosystem and for a variety of human uses, the rivers and river systems also have negative impacts. They may damage infrastructure and properties and also cause the loss of human life (Patel et al., 2016).

Flood is undoubtedly the most devastating, widespread, and frequent natural hazard of the world that produces many socioeconomic and environmental consequences within the affected floodplains. Itis the combined result of hydrological and meteorological processes that makes it one of the most destructive natural events. It is a natural phenomenon that temporary inundates surface of the land outside the water body owing to bursting and overtopping of water in the natural or artificial channel. Furthermore, rising up of ground water table due to heavy and prolonged rainfall have significant contribution to the emergence of this catastrophic events (Wisner, 2004). It is among the disastrous natural outcomes as it causes terrible and costly damage to lives including human, infrastructure, and the environment as a whole. As per the study conducted by (Abon et al., 2016) indicated, about 196 million people in more than 90 countries were exposed to catastrophic flooding problem now a day and hence it was attracting the eyes of numerous researchers all over the world. At present, flood is highly affecting worldwide people than any other catastrophic events (Banks et al., 2014).

As cited in Legese, (2022), Floods affect more people per annum than all other natural and technological disasters put together. The damage caused by floods to people and property across the planet has been extremely severe in recent decades. Flood impact tends to be very severe in African cities where urbanization has taken place with improper land use planning and lack of early warning systems. It is the second and therefore the worst environmental disaster next to the recurrent droughts in Africa. Most countries in SubSaharan Africa are exposed to at least one or multiple of the natural

hazards. Flood usually affects large river basins like the Congo, Niger, Nile, and Zambezi basins.

Flood is non-stopping and frequently occurring natural events in floodplains of monsoon rainfall areas like Ethiopia, where over 80% of annual precipitation falls in the four wet consecutive months (Billi et al., 2015). According to Abon et al. (2016), flood is one of the most harmful natural disasters in the world, and therefore, it needs excellent attention especially in the area that redundantly affected by flooding problem. The Flooding is often caused by heavy rain, snowmelt, land subsidence, rising groundwater, and dam failures. But in Ethiopia, the dominant cause of flooding is heavy rainfall (YS and Gebre, 2015).

Through extended rain falling over huge areas, the rivers are supported by a system of channels, streams, and tributaries, and flows build up to the point where the normal channel is overcome and water floods nearby areas (Assefa and Abunna, 2018). Human activities, including unplanned fast settlement development and unrestrained construction of structures at large and major land use changes, can impact the spatial and temporal array of vulnerabilities (Smit and Pilifosova, 2003). There are some factors that contribute to the overflowing problem, including topography, engineering structures, climate, poor drainage, and other local causes (Semaw et al., 2022).

Agriculture dominates the majority of the land in the Suha River's vicinity. Most of the time, particularly in the summer, the area experiences flooding. Therefore, this study will focus on flood inundation mapping of the Suha River by collecting the necessary data and analyzing it using HEC-HMS and HEC-RAS models.

1.2 Problem of the Statement

Different parts of the country are threatened by the quite unprecedented and abnormal magnitude of flooding. For instance, in 2006, quite 357,000 people were suffering from flooding and therefore the country lost about 40 million Ethiopian Birr. The problem is more acute within the river basins and concrete areas. For instance, in 2006, flooding in South Omo and Dire Dawa has killed 300 people in Dire Dawa city. Consequently, many

also are affected before the particular information is submitted to the acceptable decision-makers.

According to the latest United nation report, heavy rains across the country have seen further flooding in South Omo Valley, Dire Dawa, Amhara, Afar, Somali, Tigray, Gambella, and Oromia regions, approximately 35,000 people are displaced, 120,000 affected and 620 confirmed dead (Legese et al., 2020).

Suha watershed, located in the East Gojam zone of Ethiopia, is characterized by severe flooding. At each year flood becomes a challenging disaster and emerging issue for the local community. Especially starting from July to the mid of September, the flood inundates wide area of the riversides. Each year, the flood inundates the agricultural area up to a distance of 100m to 150m and the farmers loss from 20-30 ha of land per one km length of the river. This means the local community losses from 800 to 1200 Quntal of crop at each year.

Once more, when the river is full, it snatches away the locals' cattle. In addition to the agricultural purpose, the areas near to the river also used as grazing purpose. During heavy rainfall, the flood overtops the river channel and inundates this grazing land and damaged the domestic animals like cattle and donkeys since 2020. The flood is also affecting the transportation system of the area. It overtops the bridge which is located at the downstream and blocks the movement of vehicles for the last three years.

Therefore, this study focuses on flood inundation mapping of this watershed to minimize the flood effect on the community life and property.

1.3 Objective of the Study

1.3.1 General Objective

The main objective of this study is to conduct a flood inundation mapping of the Suha River using a one-dimensional HEC-RAS model.

1.3.2 Specific Objectives

The following specific objectives were set to achieve the main objective.

- To evaluate the performance of both HEC-HMS and HEC-RAS models.

- To prepare a flood inundation map of the flood plain area for different return periods.

1.4 Significance of the Study

To protect human life and property in the local community from hydrologic extremes, we need information on water resources, hydrological hazard characteristics, and their impact. Accurate flood inundation maps can be the most valuable tool for avoiding severe social and economic losses from floods. Timely updated floodplain maps also improve public safety by raising awareness about the flood for them as well. Early identification of flood-prone properties during emergencies allows public safety organizations to establish warning and evacuation priorities for them.

This study can give full information concerning the characteristics of the study area, peak flood magnitude and its frequency, location of the worst flood-prone area, and its extent for those who will go to take action like flood mitigation measures and decision-making. And it can also be used as a reference for researchers who intend to carry out further investigations in this study area using different techniques and more advanced tools. Finally, the result will be used as input in the processes to update plans, policies, and programs to minimize losses of human life and their properties due to flood risks in the study areas and assure community sustainability.

1.5 Scope of the study

This study will cover topics like calibration and validation of HEC RAS and HEC HMS models, computation of peak discharge at the outlet of the watershed, flood frequency analysis of the watershed at different return periods using flood frequency analysis methods (such as Gumbel and log Pearson type III methods) and the HEC HMS model, preparation of land use land cover maps, preparation of soil type maps, unsteady flow analysis, and preparation of flood inundation maps for the specified section of the river.

1.6 Research questions

- Does HEC-HMS and HEC-RAS models perform good in Suha watershed to use for flood plain analysis?
- How much area will be inundated at different return periods?

2. LITERATURE REVIEW

2.1 Introduction

A flood is an unusually high stage in a river, normally the level at which the river overflows its bank and inundates the adjoining area. The damages caused by floods in terms of loss of life, property, and economic loss due to disruption of economic activities are all too well known (Patel et al., 2016).

River flooding has been defined as "a general and temporary condition of partial or complete inundation of normally dry land areas from the usual and rapid runoff of surface waters from rainfall"(Hua, 2014). Flood is used in a broader sense to cover several river activities that cause damage, i.e., inundation of floodplains and adjacent terraces, bank cutting, river channel shifting, and debris torrents during normally high discharge (UNDRO'S and Nations, 1991). Flood has substantial impacts on human activities such as; it can intimidate people's lives, their property and the environment. Resources damage at flood risk may include housing, transport and public service infrastructure, commercial, industrial and agricultural enterprises (Sisay and Awoke, 2015).

2.2. Types of Flood

i) Flash flood

These floods are frequently related to violent convection storms of brief duration falling over a small area. Flash flooding can occur in almost any area where there are steep slopes, but it is commonest in mountain districts subject to frequent severe thunderstorms. Flash floods are often the result of short-lived heavy rains. This particular sort of flooding commonly washes away houses, roads, and bridges over small streams, which then has a critical impact on communities and transport in these often-remote areas. Flash floods are defined as those flood events where the increase in water occurs either during or within a couple of hours of the rainfall that produces the increase and occurs within small catchments where the reaction time of the catchment area is brief (Gaál et al., 2012). Many hydrological factors have relevance to the occurrence of a flash flood: terrain gradients, soil type, vegetative cover, human habitation, and antecedent rainfall (Legese et al., 2020). Flash floods are those formed by excess rain falling on

upstream watersheds and gushing downstream with massive concentration, speed, and force (Legese et al., 2020)

ii) River flood

River flooding is happening over a good range of rivers and catchment systems. Floods in river valleys occur totally on flood plains or wash lands as a result of flow exceeding the capacity of the stream channels and spilling over the natural banks of artificial embankments. River floods, in contrast to flash floods, typically unfold over days or maybe months (Legese et al., 2020).

The characteristic features of floods expressed by a hydrograph are maximum discharge, the duration of the flood rise and recession phases, the entire volume of a flood, and flood asymmetry, expressed as a ratio of flood rise to a recession. The inundation caused by a flood, its scale, and its consequences for nature and humans depend upon the flood rise rate maximum discharge, and duration (Mandych, 2005). The flood type that affects my study area is a riverine flood.

iii) Urban flooding

Urban flooding is intensified by dramatic changes within the impervious area, in addition to heavy rainfall and extreme climatic events. Urban flooding occurs when intense rainfall within towns and cities creates rapid runoff from paved and built-up areas, exceeding the capacity of storm drainage systems. In low-lying areas within cities, the formation of ponds from runoff occurs not only owing to high rainfall rates but also due to drainage obstructions caused by debris blocking drainage culverts and outlets, actually because of a lack of maintenance (Legese et al., 2020).

In Ethiopia, urban flood incidents have become a significant problem in recent years. They are mainly related to poorly designed urban systems and land use planning. Combined therewith, the lack of an early warning system and arranged flood disaster mitigation measures at the national and native levels further increases the gravity of the matter. Urban floods are more costly and difficult to manage (Demessie, 2007). While rural flooding may affect much larger areas of land and hit the poorest section of the population, the impacts of urban floods are characteristic therein the concentration of population within the urban environment is typically much higher. Therefore, the damage

is more intense and typically more costly. Construction of roads and buildings also acts to extend runoff and results in an increased likelihood of localized urban flooding (Ouma and Tateishi, 2014).

2.3 Flood Causes and Consequences

2.3.1 Natural causes

Rainfall is the dominant cause for creating a flood, but there are many other contributing factors. When rain falls on a catchment, the quantity of rainwater that reaches the waterways depends on the characteristics of the catchment, particularly its size, shape, and land use. Some rainfall is captured by soil and vegetation, and therefore the remainder enters waterways as flow. River characteristics like size and shape, the vegetation in and around the river, and therefore the presence of structures in and adjacent to the waterway all affect the extent of water within the waterway (Jacinto et al., 2015).

2.3.2 Anthropogenic causes

A flood may be a natural disaster. However human activities in many circumstances change flood behavior. Activities within the catchment like land clearing for agriculture may increase the magnitude of a flood which increases the damage to the properties and life. Intensive agricultural activities on steep slope areas of the catchment and its expansion decrease the abstraction of rainwater and thereby changed quickly to flood water (Bishaw, 2012). Deforestation of forests and urbanization are the main causes of rapid increase within the flow of rivers, giving rise to floods. Reservoir construction, additionally to changing river flow regime also can trigger a variety of other negative consequences that promote flooding (Legese, 2022).

2.3.3 Consequences of Flooding

Floods impact on both individuals and communities, and have social, economic, and environmental consequences. The results of floods, both negative and positive, vary greatly counting on the situation and extent of flooding, and therefore the vulnerability and value of the natural and constructed environments they affect (Jacinto et al., 2015). The adverse health impacts of flooding are very complex. One of the health impacts of flooding is death. Deaths caused by flooding can occur in different ways and periods, but

the most easily recognized ones are due to drowning and injuries obtained during the onset of flooding. Injuries can happen before, during, and after flooding. Injuries occur before flooding when people are trying to escape the approaching water (Greenough et al., 2001).

People also are injured during the onset of floods primarily when they are hit by an object in fast flowing water (Ahern & Kovats, 2006). Once the flood waters recede people can still be injured when they return to their homes and business areas and start to clean up the damage. In addition to the escalating probability of death and injuries, floods also cause an increase in the transmission of diarrheal disease. The incidence of diarrhea is linked to floods because flood waters often carry pathogens and pollutants that can contaminate food and water source (Hunter, 2003). Diarrhea is not the only disease that results from flooding. Vector-borne diseases such as malaria also increase in the aftermath of floods. This is due to an increase in the habitats, such as stagnant pools, used by the vector population (Ahern et al., 2005).

The effects of a flood on the inundated land and therefore the property located there will differ, counting on local factors and conditions, and where the flood originates. The most effects are from an accumulation of water and therefore the dynamic impact of flowing water during the movement of a flood wave. In specific conditions, the consequences of a flood depend upon an outsized number of additional circumstances, like depth and duration of inundation, the velocity of the flood's wave movement along with the river, height and velocity wave travel, then forth (Legese, 2022).

2.4 Flood prone areas in Ethiopia

In flood-prone areas, understanding flood causing factors can increase the knowledge, awareness, and individual initiatives to guard themselves and their properties using appropriate flood management measures before and through flood events (Erena & Worku, 2018). Much of the flood disasters in Ethiopia are attributed to rivers that overflow or burst their banks and inundate downstream plane lands. The flood that has recently assaulted Southern Omo Zone and East Shewa Zone may be a typical manifestation of river floods.

Therefore, due to its topographic and altitudinal characteristics, flooding, as a phenomenon, is not new for Ethiopia. They have been occurring at different places and times with varying magnitude. Some parts of the country do face major flooding. Most prominent ones include extensive plain fields surrounding Lake Zeway and Meki in Oro mia Regional State; areas in Oromia and the Afar Regional States that constitute the mid and downstream plains of the Awash River; places in Somali Regional State that fall mainly along with downstream of the Wabishebelle, Genalle and Dawa Rivers; low-lying areas falling along Baro and Akobo Rivers in Gambella Regional State; downstream areas of Omo River within the Southern Nations, Nationalities and Peoples Regional State (Legese et al., 2020).

2.5. Hydrologic Analysis of Flood Modelling

According to Burrell et al. (2015) manual stream flow measurements for determining a flood frequency relationship at or near a site are usually unavailable. In some cases, it is a well-known practice to determine the peak runoff rates and hydrographs through using statistical and empirical methods. In common, results from using a number of methods should be compared. The discharge which reflects best in the local project conditions through the reasons documented should to be used.

2.5.1 Rational method

The Rational Method provides estimates of peak runoff rates for small urban and rural watersheds of less than 50 hectares (0.5 square km) and in which natural or man-made storage is small. It is best suitable to the design of urban storm drainage systems, small side ditches and also median ditches with driveway pipes. This should be used with restraint if the time of concentration exceeds 30 minutes and here rainfall is a basic input for this technique of flow estimation (Pilgrim, 1976).

2.5.2 SCS Method

The Soil Conservation Service advanced the runoff curve number technique as a means of determining the amount of rainfall existing as runoff. This technique should to be used if and only if when the watershed has unique main channel or when there are two main channels which have approximately equivalent times of concentration; unless, a

hydrograph technique should be used. Other different methods may also use when the channel or reservoir routing is required and/or where watershed storage is either greater than five percent or located on the flow path that used to calculate (Srinivasan and Arnold, 1994).

2.5.3 Flood Frequency Analysis

Hydrologic processes such as floods are exceedingly complex natural events. They are resultants of a number of component parameters and are therefore difficult to model analytically. For example the flood in a catchment depend up on the characteristics of the catchment, rainfall and antecedent moisture condition, each one of these factors in turn depend upon a host of constituent parameters. This makes the estimation of the flood peak a very complex problem leading to many different approaches.one of these is statistical method of frequency analysis. The most commonly used distribution functions are: Gumbel's extreme-value distribution, log-Pearson type III distribution and log normal distribution (Okonofua et al., 2022)

2.5.4 Regional Regression Equation

When the available data at a catchment is too short to conduct frequency analysis, a regional analysis is adopted. In this a hydrological homogeneous region from the statistical point of view is considered. Available long-time data from neighboring catchments are tested for homogeneity and a group of station satisfying the test is identified. This group of station constitutes a region and all the stations data of this region are pooled and analyzed as a group to find the frequency characteristics of the region (Hosking and Wallis, 1997).

2.6 Hydrologic and Hydraulic Flood Modelling

2.6.1 Model and Software Selection

The selection of the best and most appropriate software is an essential part of any research project. The choices of software for a specific hydrological situation have implications for water resource planning, development, and management. There are various criteria for choosing the most suitable software. The choice depends mainly on the requirements and needs of the research or project under consideration. The following

are among the factors and criteria involved in the choice of software: Required output of the software, Availability of input data, Prices and availability of the software, the software structure, the lengths of the records of the various types of data, and the like (Sinha et al., 2014)

2.6.2 Hydrologic Model (HEC-HMS)

HEC-HMS is hydrologic modeling system software developed by the USACE HEC. It is the physically-based and conceptually semi-distributed models are intended to compute the rainfall runoff process in a wide range of geographic areas, from large river basins, water supply, and flood hydrology to small urban and natural watershed runoff. Hydrographs created by the program can be used directly or in conjunction with other software for the study of water availability, flow forecasting, urban drainage, future urbanization effects, reservoir spillway design, floodplain regulation, flood damage reduction, wetlands hydrology, and systems operations. The software is designed for interactive use in a multi-tasking, multi-user network environment and can be utilized with both XP and Microsoft Windows (Shende, 2006).

The advantages of using HEC-HMS are that it draws on more than 30 years of experience in hydrologic simulation. It is freely available for download from the HEC website and is supported by the US Army Corps of Engineers. It provides a graphical user interface, making it easier to use the software, and the program is broadly used and accepted for many official purposes, such as floodway determination for the FEMA (Federal Emergency Management Agency) (Charley, 1995).The main inputs to the model are the watershed stream network and size, infiltration, and loss method, transform method for transforming excess precipitation into runoff, routing methods (i.e., Muskingum, Kinematic Wave, Lag, Modified Puls, Muskingum-Cunge, and Straddle Stagger), meteorological data (i.e., precipitation), and the time span of the simulation. The outputs from the model include the hydrographs and flow volume (Yuan and Qaiser, 2011b).

i) HEC-HMS technical capability

There are four model setups that require specification in the execution of a simulation or run. The first model setup is the basin model, which encompasses parameters and data connectivity for hydrological elements such as sub-basin, routing of reach, junction,

reservoir, source, sink, and diversion. The second model setup is the meteorological model, which consists of meteorological data and the information needed to process it. The model may represent historical or hypothetical conditions. The third model setup, called Control Specifications Manager, specifies time-related information for a simulation. The fourth one is time series data, which is used to insert precipitation, streamflow, and other data. A project is used to hold the different data sets and can contain many of each type. The program is multi-platform capable, meaning it operates on more than one kind of computer operating system (Brandon, 2016 ; Merwade, 2007).

ii) HEC-HMS parameters

The HEC-HMS model requires three main input process parameters. Among them is the precipitation loss method for overland flow, which accounts for the infiltration losses. There are multiple methods available in HMS, including SCS Curve Number, Initial and Constant, Deficit and Constant, Exponential, Green-Ampt, Smith Parlange, and Soil Moisture Accounting (Yuan and Qaiser, 2011a). After the precipitation losses are accounted for, a transform method must be specified for transforming overland flow into surface runoff. The different methods available for the transform method in HMS are SCS unit hydrographs, Clark or Snyder unit hydrographs, kinematic waves, ModClark, and user-specified unit hydrographs. There are many techniques available in HMS for routing stream flow. These are Kinematic Wave, Lag, Modified Puls, Muskingum, Muskingum-Cunge, and Straddle Stagger. The Muskingum method is the most recommended one (Arsenault et al., 2018). The different parameters in the Muskingum method are K, X, and the number of sub-reaches (n), which need to be specified. Muskingum K is the travel time through the reach, which ranges from 0.1 to 150 hours. Muskingum X is the weighting between inflow and outflow influences; it ranges from 0 to 0.5. The number of sub-reaches affects attenuation; one sub-reach gives more attenuation, and increasing the number of sub-reaches decreases the attenuation (Yuan and Qaiser, 2011b).

iii) HEC-HMS components

HEC-HMS model components are used to compute or simulate the hydrologic response in the watershed. It includes basin models, meteorological models, control specifications,

and input data. A simulation calculates the precipitation-runoff response in the basin model, which is given input from the meteorological model. The control specifications define the period of time and time steps of the simulation run. Input data components, such as time-series data, paired data, and gridded data, are often needed as parameters in basin and meteorological models (Arsenault et al., 2018).The four main components of HEC-HMS are the basin model manager, the meteorological model manager, the control specifications manager, and the input data time series manager.

The basin model manager represents the physical watershed. The user develops a basin model by adding and connecting hydrologic elements. It is based on a graphic user interface (GUI) and can import map files from the GIS environment through an Arc GIS extension called HEC-Geo HMS to use as background map files later in the hydrologic modeling process (Fleming and Brauer, 2016b). The precipitation and evapotranspiration data necessary to simulate watershed processes are stored in the meteorological model manager. The meteorological model manager calculates the precipitation input necessary for each sub-basin element. This model can make use of both points and gridded precipitation and has the capability to model frozen and liquid precipitation along with evapotranspiration (Fleming and Brauer, 2016b). An evapotranspiration method is only required when simulating the continuous or long-term hydrologic response in a watershed. The meteorological component is also the first computational element utilizing which precipitation input is spatially and temporally distributed over the river basin (Gebre, 2015). The control specifications are defined as the time-related information in the simulation, including the starting dates, ending dates, and the computational time interval. The function of control specifications is to set the starting and ending dates, times, and time (computation) intervals. The time step for HEC-HMS model calibration for the catchment is divided into different time steps for calibration, simulation, and verification (Hamdan et al., 2021).

2.6.3 Hydraulic Model (HEC-RAS)

HEC-RAS is an integrated system of software designed for interactive use in a multitasking, multi-user network environment. The system is comprised of a graphical

user interface (GUI), separate hydraulic analysis components, data storage and management capabilities, graphics, and reporting facilities (Goodell and Brunner, 2004). The HEC-RAS software supersedes the HEC-2 river hydraulics package, which was a one-dimensional, steady-flow water surface profile program. The first version of HEC-RAS was released in July 1995.

Steady flow surface profiles are used for the calculation of water surface profiles for steady, gradually varied flow. The system can handle a single river reach, a dendritic system, or a full network of channels. The steady flow component is capable of modeling subcritical, supercritical, and mixed flow regime water surface profiles (Kumar et al., 2011). The basic computational procedure is based on the solution of the one-dimensional energy equation. Energy losses are evaluated by friction (Manning's equation) and contraction/expansion (coefficient multiplied by the change in velocity head). The momentum equation is utilized in situations where the water surface profile is rapidly varied. The unsteady flow simulation component of the HEC-RAS modeling system is capable of simulating one-dimensional unsteady flow through a full network of open channels. The unsteady flow component was developed primarily for subcritical flow regime calculations (Mignot et al., 2006).

Awal (2003) compared steady and unsteady flow analysis using HEC-RAS. He observed that the water surface elevation computed by the unsteady model was less than that computed by steady flow analysis, and the flooded area was about 2.84% larger in the case of steady analysis. He also prepared a flood inundation map based on the gradually varied steady flow analysis using HEC-RAS of different year return periods floods and also mapped the settlement area under high hazard zones. Shrestha et al. (2020) assessed the flood inundation problem in Blakhu Khola using Steady flow analysis which shows barren area near the river is susceptible to flood hazard, which indicates future human lives are more prone to disasters as those lands have gone through planning for future settlement.

2.6.4 ARC-GIS

A geographic information system is a rapidly developing tool with a range of applications. GIS is defined as computer systems capable of assembling, storing, manipulating, and displaying geographically referenced information (Flax et al., 2002). The power of GIS lies in its tremendous clarity of presentation and analysis. It has the ability to take scattered, confusing data and represent its spatial relationship in such a way that researchers can realize new levels of understanding. In the context of flood hazard management, GIS can be used to create interactive map overlays that clearly and quickly illustrate which areas of a community are in danger of flooding. Such maps can then be used to coordinate mitigation efforts before an event and recovery after it. GIS, thus, provides a powerful and versatile tool to facilitate fast and transparent decision-making (Raford and Ragland, 2004; Tran et al., 2009).

2.6.5 Global positioning system (GPS)

The Global Positioning System (GPS) is a satellite-based navigation system made up of network of 24 satellites (NAVSTAR Series) placed into orbit by the U.S. Department of Defense to determine the position of a feature on the earth's surface. GPS was originally intended for military applications, but in the 1980s, the government made the system available for civilian use. GPS works in any weather condition, anywhere in the world, 24 hours a day. GPS satellites circle the earth twice a day in a very precise orbit and transmit signal information to the earth. GPS receivers take this information and use triangulation to calculate the user's exact location (Manandhar, 2010).

2.7 Flood Inundation Mapping

A flood inundation map is a set of maps that shows where flooding may occur over a range of water levels in the community’s local stream or river. Inundation mapping is performed on a RAS mapper using flood hydrographs and a digital elevation model of the area. It shows the extent of the flood in the area nearest to the river. It is the basis for the conceptual flood mitigation measures. For proper flood risk management and flood damage rehabilitation, flood extent area identification is a prerequisite that can be done through flood inundation mapping (Awal, 2003; Flax et al., 2002; Taubenböck et al., 2011).

According to Merz et al. (Merz et al., 2007), flood inundation mapping is the useful tool assisting for flood hazard management and flood extent area identification. HEC-RAS is the best computer programming software widely applicable for the successful flood inundation mapping. Several critical parameters are required for performing flood inundation mapping using HEC-RAS. These are topographic data, discharge data (profiles), Manning's roughness coefficient, and river geometric cross-section (such as river centerline, flow path lines, river bank lines, XS cut line), bridge data, and physical watershed parameters (Banks et al., 2014). Flood inundation mapping requires forecasting of the behavior of stream flow and hydrological events along the flood plain under question for various recurrence intervals and the knowledge to convert the forecasted peak flood into the plan-view extent of the floodplain (Romali et al., 2018).

2.8 Flood Mitigation Measures

There are two of the most widely used flood mitigation strategies: The first strategy is the structural strategy, which is completely based on the application of engineering and technology. It is the physical structure constructed along the flood plain at the side of the river bank to avoid flood overflow. The second flood mitigation strategy is the conceptual or non-structural flood mitigation strategy, which mainly encompasses flood time computation and early flood warning systems. Owing to financial capacity, the implementation of the former flood mitigation strategy is difficult in developing countries like Ethiopia, while the latter is the only option where the construction of a structural mitigation strategy is not possible (Gilard, 1996; Hansson et al., 2008; Namara et al., 2022).

3. MATERIALS AND METHODS

3.1 General Description of the Study Area

3.1.1 Location

The study area, Suha River, is located in Enemay Wereda, East Gojjam Zone, Amhara Region, Ethiopia, at a distance of 265 km from Addis Ababa and 223 km from the regional capital city, Bahir Dar. Geographically, it is located at a latitude of 10^{o} 6' 29" to 10^{o} 41' 23" N and a longitude of 38^{o} 1' 29" to 38^{o} 20' 33" E, with an elevation ranging from 1038 to 3975 meters above mean sea level. The river section that is selected for this study is bounded by four kebele: Yensicha kebele at the upper right side, Yedeb kebele at the lower right side, Qecher kebele at the upper left side, and Guacher kebele at the middle left side. The river originates from Misrak Washa Mountain and join to Blue Nile River.

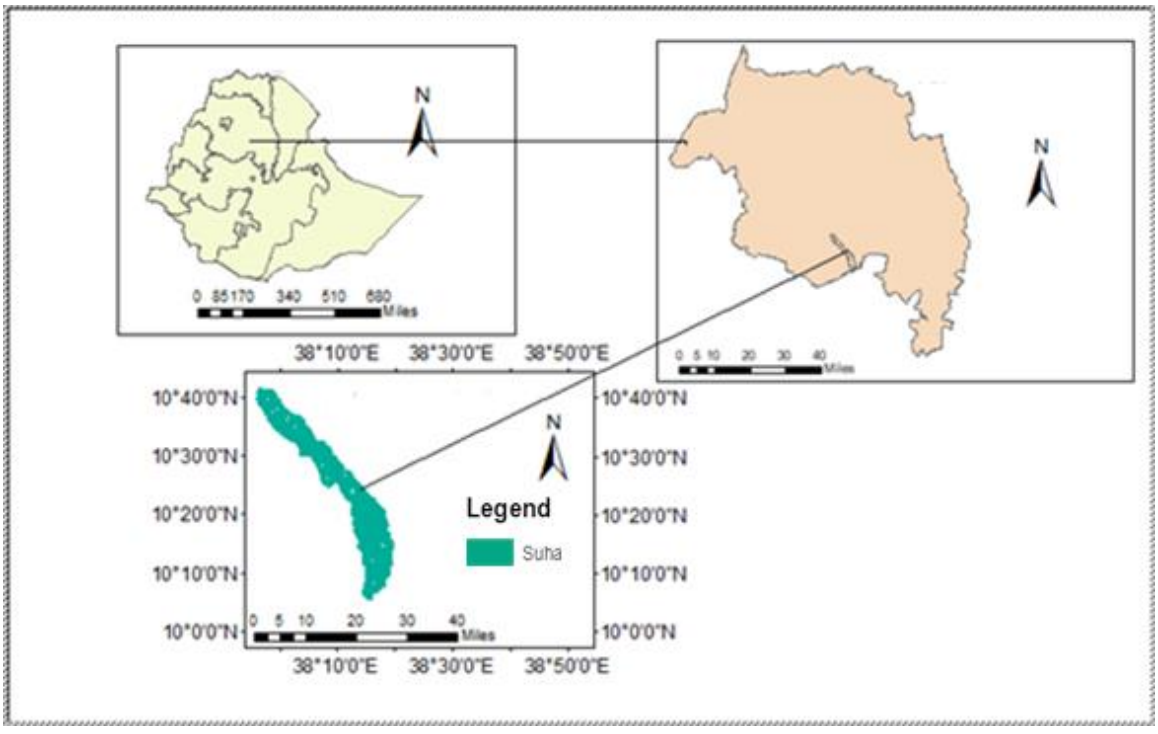

Figure 3.1: Geographical location of Suha Watershed

3.1.2 Land use and land cover (LULC)

In the study area, several indigenous tree species are found, even if their abundance is very limited. A few are found on some farmers' farmlands, river basins, around churches,

and on homesteads. The most dominant tree species in the study area was the Eucalyptus tree. This is because it grows very fast and has high economic value, such as in house construction and fuel wood. Regarding the land use and land cover pattern of the study area, of the total area of the watershed (664.8 sq. km), cultivated land covers the maximum area, which is 66.2%, and the rest are summarized in the Table 3.1.

Table 3.1 Land use and land cover of Suha watershed

Land use type	Area(sq km)	Area (%)
Cultivated land	440	66.2
Grass land	172.5	25.9
Forest land	28.1	4.2
Shrub and bush land	17.6	2.6
Built up area	6.6	1.0
Total	664.8	100

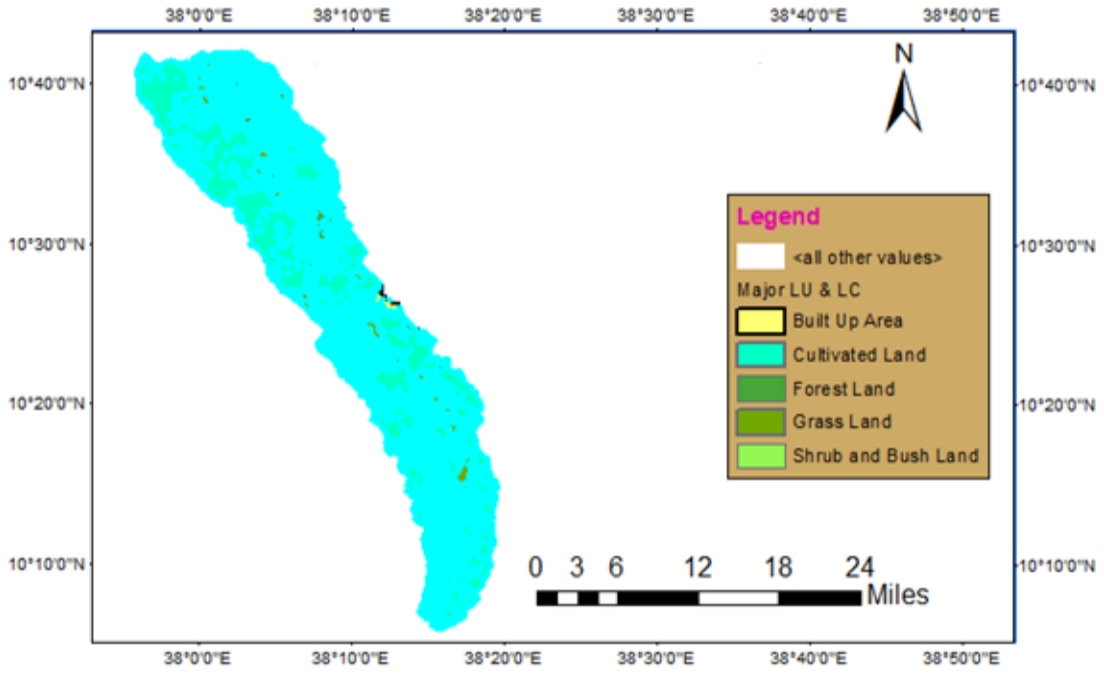

Figure 3.2: Land use and Land cover map of Suha watershed

3.1.3 Soil type of the catchment

Regarding the soil type of the study area, there are seven different types of soil. This result is obtained by clipping an Ethiopian soil map using the Suha watershed shape file

as a clip feature and an Ethiopian soil map as input feature. From the total area of the watershed, the maximum area is covered by vertisol, which is 49.1%, and the area coverage of the remaining soil types is shown in the Table 3.2.

Table 3.2 Major soil type of Suha watershed

Soil type	Area(km^2)	Area(%)
Rock surface	18.5	2.8
Vertisol	326.4	49.1
Nitosols	56.2	8.5
Luvisols	70.2	10.6
Lithosols	117.2	17.6
Rendzians	60.8	9.1
Cambisols	15.5	2.3
sum	664.8	100

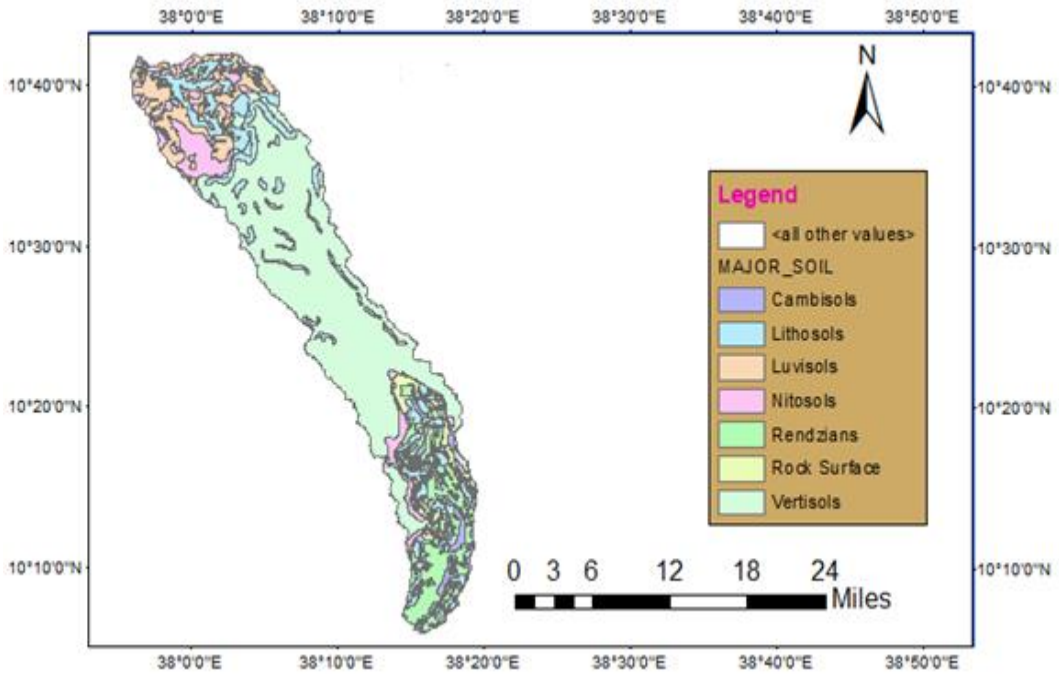

Figure 3.3: Soil type of Suha watershed

3.1.4 Rainfall

Rainfall mainly comes from June to September, when the Inter-tropical Front, the zone of convergence of winds, is located to the north of the country. During this time of the year, moist winds from the middle part of the Atlantic Ocean, often referred to as Equatorial

Westerlies, are down towards this area of low atmospheric pressure, providing rain. Thus, most of the western parts and the highlands that are situated on the direct path of the moist winds capture more rainfall than the rest of the regions. The rainfall pattern is unimodal, with a rising limb starting in May and reaching a peak between July and August. More than 75% of the total rain falls in June, July, August, and September (locally known as kiremt season) (Wakjira et al., 2021).

In general, the region enjoys a mean annual rainfall in excess of 1200mm. The mean annual rainfall over the whole region varies from 1189mm in the east to well over 1711mm in the west. The amount of rainfall, as well as the length of the rainy season, decreases northward and north-eastward from the south-western corner of the region (Geremew et al., 2020).

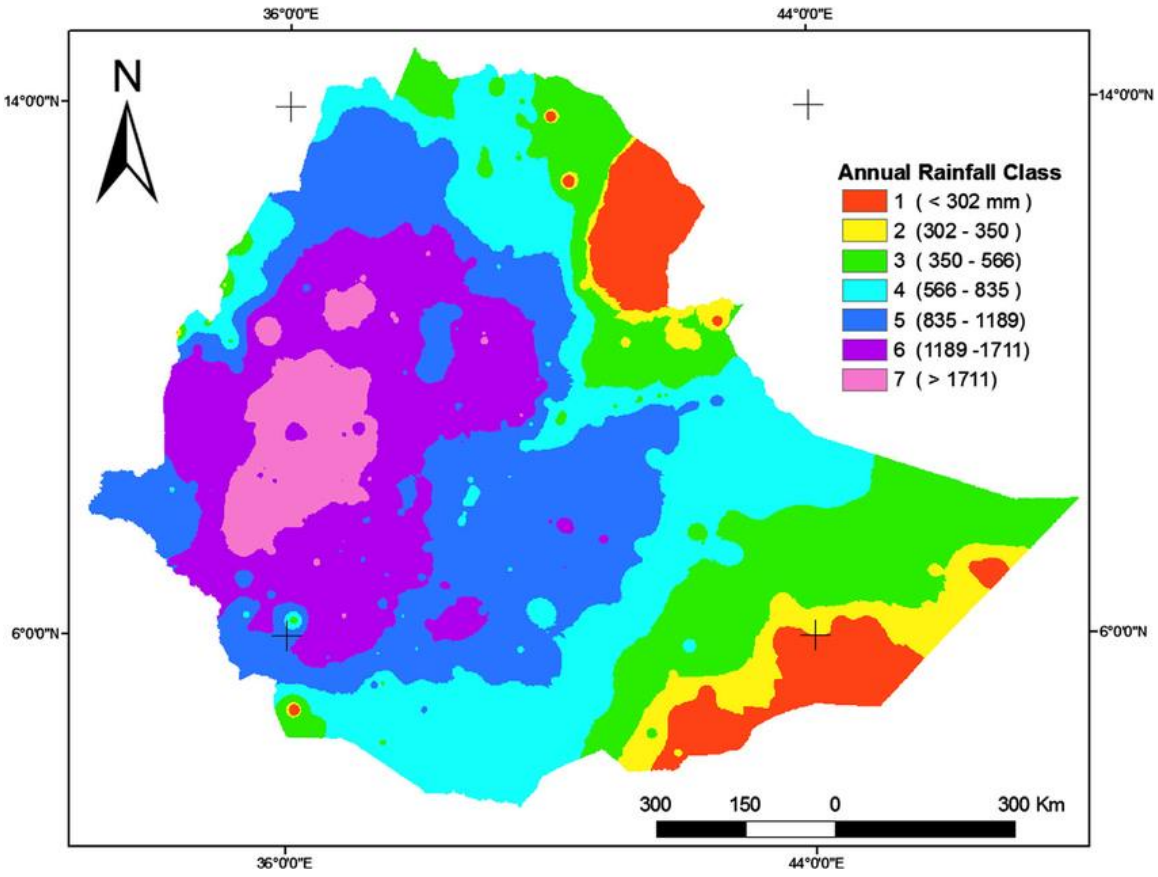

Figure 3.4: Spatial variability of the mean annual rainfall in Ethiopia (Source: www.researchgate.net)

3.1.5 Climate

The study area is characterized by sub-humid climatic conditions and typically represents the "Weynadega" zone of the traditional agro-climatic classification system of Ethiopia. The climate is generally humid. As measured at the Bichena weather station, the mean annual temperature is 19.750 °C, with a minimum temperature of 14.5°C in August and a maximum temperature of 25 °C in May (Bureau, 1997).

3.2 Materials used

Tape: to measure the distance between stations and the width difference at each station for cross-sectional data collection.

Camera: to capture the data collection system in the field.

Total station: to measure the elevation, latitude, and longitude of each station.

Reflector: to identify the place that we need to take reading by setting the reflector on a place.

3.3 Data collection methods

To achieve the specified objective of this study, both quantitative and qualitative data were collected. The data were collected from two main sources: primary and secondary sources of data. The primary sources of data include field observations, field surveys and measurements, and interviews, whereas the secondary sources of data are journals, books, previous related work, and different organizations.

3.3.1 Primary data collection

3.3.1.1 Field measurement

The total distance taken for this specific study was 4.6 km, taking into account the middle reach of the river. The bottom width of the river ranges from 5 to 15 meters, and the top width ranges from 15 to 20 meters. The distance between each cross-section was not equal because the morphology of the river was not the same. The interval taken between each station at straight reach and meandering reach was not the same. At straight reach the data was collected at wider interval, while for a reach not straight shorter interval of distance was taken. River cross section data at different stations surveyed and the sample

cross section profiles of the river are shown in Figure. 3.5. The longitudinal river profile of the selected reach and sample photos taken during field data collection are also shown in Figures 3.6 and 3.7, respectively.

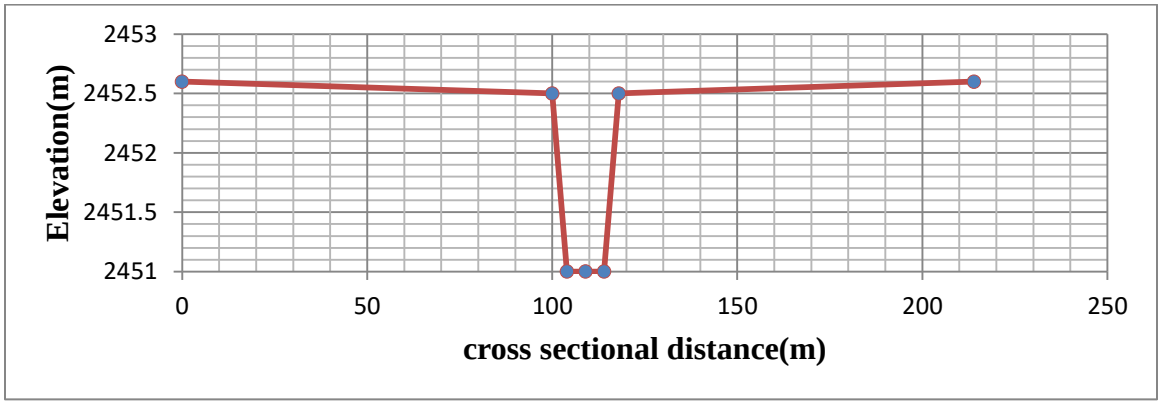

Figure 3.5: Sample cross section profiles of Suha River

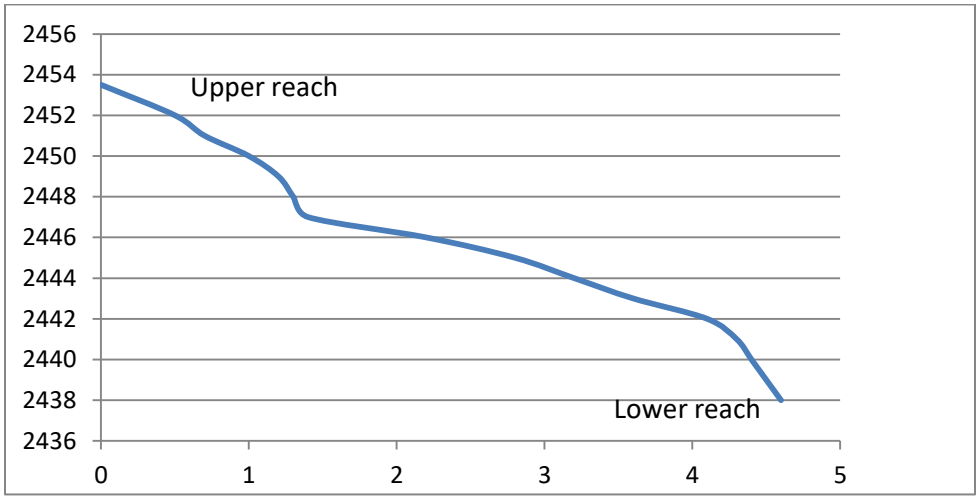

Figure 3.6: The longitudinal river profile of the selected reach

(a)

(b)

Figure 3.7: Sample photos during field data collection: (a) May20, 2014 E.C (b) July1, 2014 E.C

3.3.2 Secondary data collection

3.3.2.1 Rainfall data

The rainfall data is collected from the Ethiopian National Meteorological Agency for neighboring stations in the study area. The stations that are nearest to the study area are known using ARC-GIS. First, a Thiessen polygon was made for Ethiopian national meteorological stations, and then the Thiessen polygon was clipped using the shape file of the watershed as the clip feature and the Thiessen polygon as the input feature. So the nearest and surrounding stations are Bichena, Felege Birhan, Debrewerk, Sheble Berenta, and Yetemen. Among these five stations, Bichena contributes the maximum area almost 31.8 % around 211.6 km2, and the remaining station Yetemen, Debrewerk, Felege

Birhan, and Shebleberent covers 136.7 km^2, 159.4 km^2, 139.3 km^2, and 17.8 km^2, respectively, as shown in the Table 3.3.

Table 3.3 Station name and their coverage area

station name	long	lat	alt	Mean annual rainfall(mm)	area(km^2)	coverage area (%)
Yetimen	38.1466	10.3291	2418	1186.5	136.7	20.6
Bichena	38.2035	10.4448	2532	947.2	211.6	31.8
Debere Work	38.1623	10.6506	2508	909.7	159.4	24.0
Felege Birihan	38.0671	10.7427	2710	920.1	139.3	21.0
Shebeleberenta	38.3437	10.4449	2375	1180.8	17.8	2.7
				SUM	664.8	100

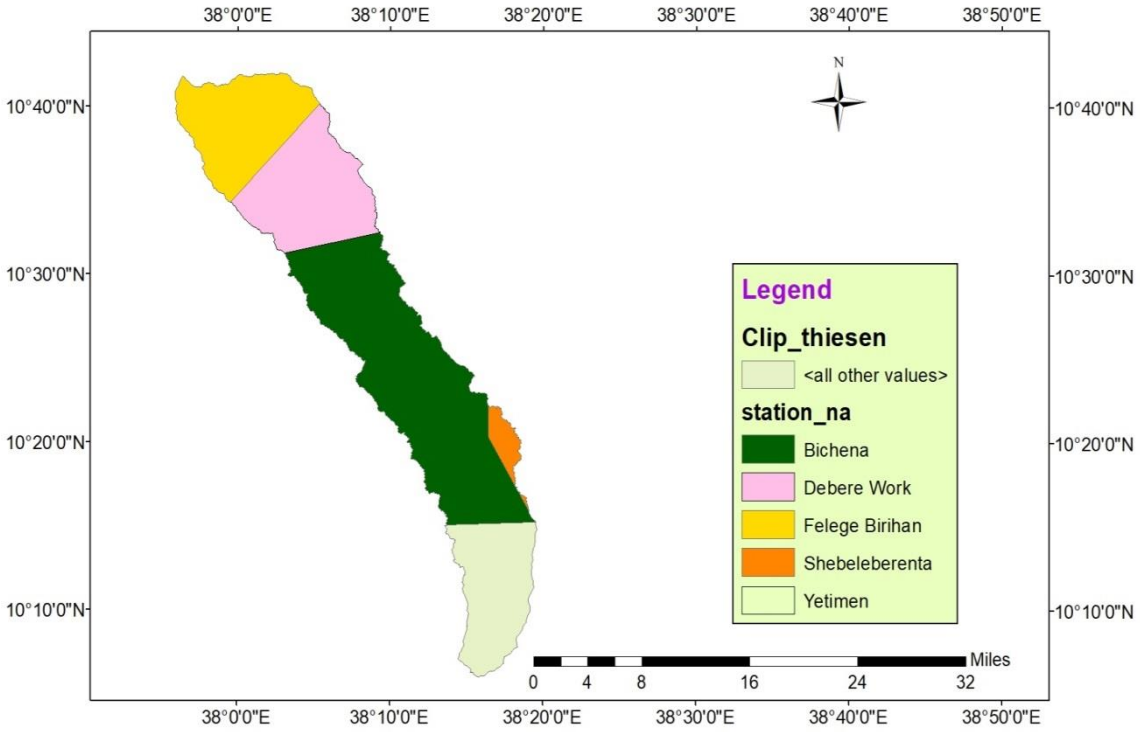

Figure 3.8: Nearby meteorological station within Suha watershed

3.3.2.2 Hydrological data

The stream flow data is used for different purposes, such as calibration and validation, predicting the flood for different return periods, and analyzing the past maximum flood

occurrence. In this study, the available daily discharge data are collected from the Abay Basin Authority. The gaging station of the study area is located between Bichena and Yetemen towns, and the available annual flow data and mean monthly flow data are summarized in the Table 3.4.

Table 3.4 Annual stream flow of Suha River

year	Annual flow(m^3/s)	Mean monthly flow(m^3/s)
1986	1583.1	131.9
1987	933.6	77.8
1988	1514.6	126.2
1989	1019.8	85
1990	683.4	57
1991	1231	102.6
1992	1123.4	93.6
1993	1172.6	97.7
1994	1312.6	109.4
1995	898.2	74.9
1996	1116.6	93
1997	1044.3	87
1998	1566.3	130.5
1999	1039	86.6
2000	121.9	10.2
2001	444.1	37
2002	849	70.7
2003	1240	103.3
2004	724.6	60.4

3.3.2.3 Digital elevation model (DEM)

It is the digital representation of the land surface with respect to any reference datum, and it is used as an input for ARC-GIS software for watershed delineation and estimation of catchment characteristics. The lower and higher elevations of the study area are 1038 m and 3975 m, respectively.

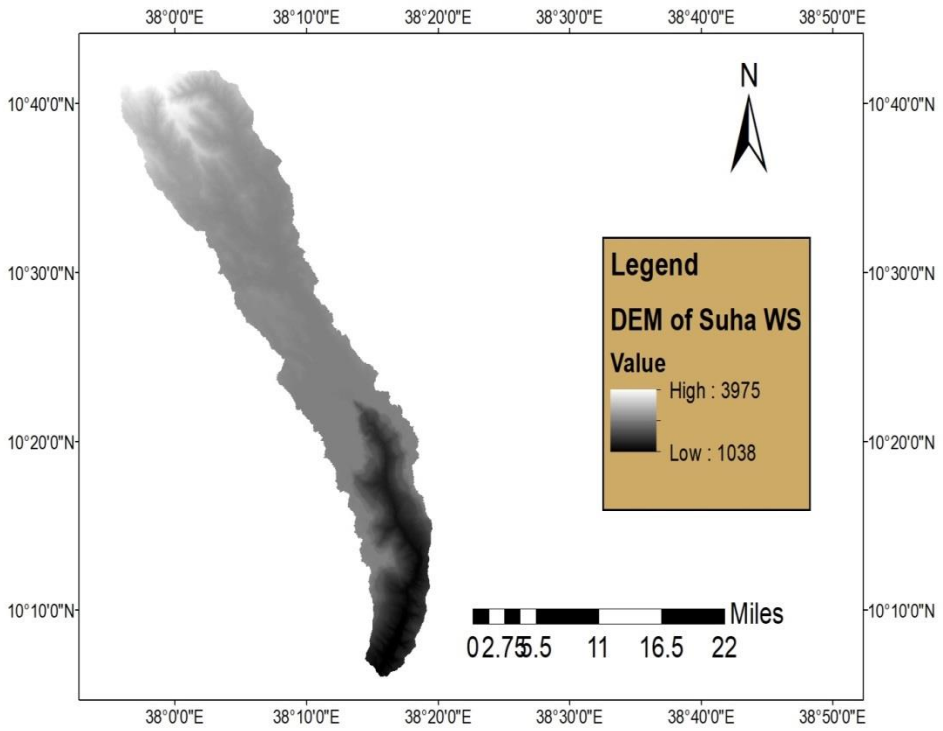

Figure 3.9: DEM of Suha watershed

3.3.3 Summary of the data type, source and purpose

For this specific study, the data mentioned in the table below are used for analysis and running the models for preparing the flood map. Hence, each data point's source and purpose are shown in Table 3.5.

Table 3.5 Data types and sources

Types of data	Source of data	Purpose of data
Rainfall data	NMA Addis Ababa, Ethiopia	For HEC-HMS model
Hydrological data	Abay Basin Authority Bahirdar, Ethiopia	For calibration and validation
DEM data	USGS earth explorer	To delineate the watershed For digitizing on HEC-RAS
Land use & land cover	Amhara design & supervision	To prepare CN
Soil type data	MoWIE Addis Ababa, Ethiopia	To prepare CN
Survey data	Field survey	For input to HEC-RAS Simulation

3.4 General frame work for Preparing Flood inundation map of Suha watershed

In this specific study, in order to prepare a flood inundation map, both hydrologic and hydraulic modeling were used. Hence the hydrologic modeling (HEC-HMS) used to prepare flood frequencies for water surface simulation and flow hydrographs for upstream boundary conditions. As shown in Figure. 3.11, the thesis work comprises both hydrological and hydraulic models. Therefore, the general framework figure shows the steps followed in this specific thesis work and how the data collection methods, data analysis, and results integrated and followed one another. For the sake of verification of the models, both calibration and validation are performed. Land use, land cover, and soil type data are used for the preparation of the curve number, which is directly used as an input for the HEC-HMS model simulation.

In hydraulic modeling (HEC-RAS) simulation, the steps followed were digitizing the river center line, cross-sectional cut lines, bank lines, and flow path center lines. Following it, the surveyed river cross section is required as an input for hydraulic modeling in HEC-RAS simulation. After that, flood area generation, editing geometric data, setting Manning roughness, setting boundary conditions, setting contraction/expansion coefficient, and finally importing and editing flow data for different return periods. For hydrological modeling calibration and validation, hold on by comparing the HEC-HMS model simulation value with the recorded observed one. To approximate the simulated and recorded values, it was better to change and adjust the curve number value. This process continues until the required result is obtained and the model performance efficiency value is satisfied.

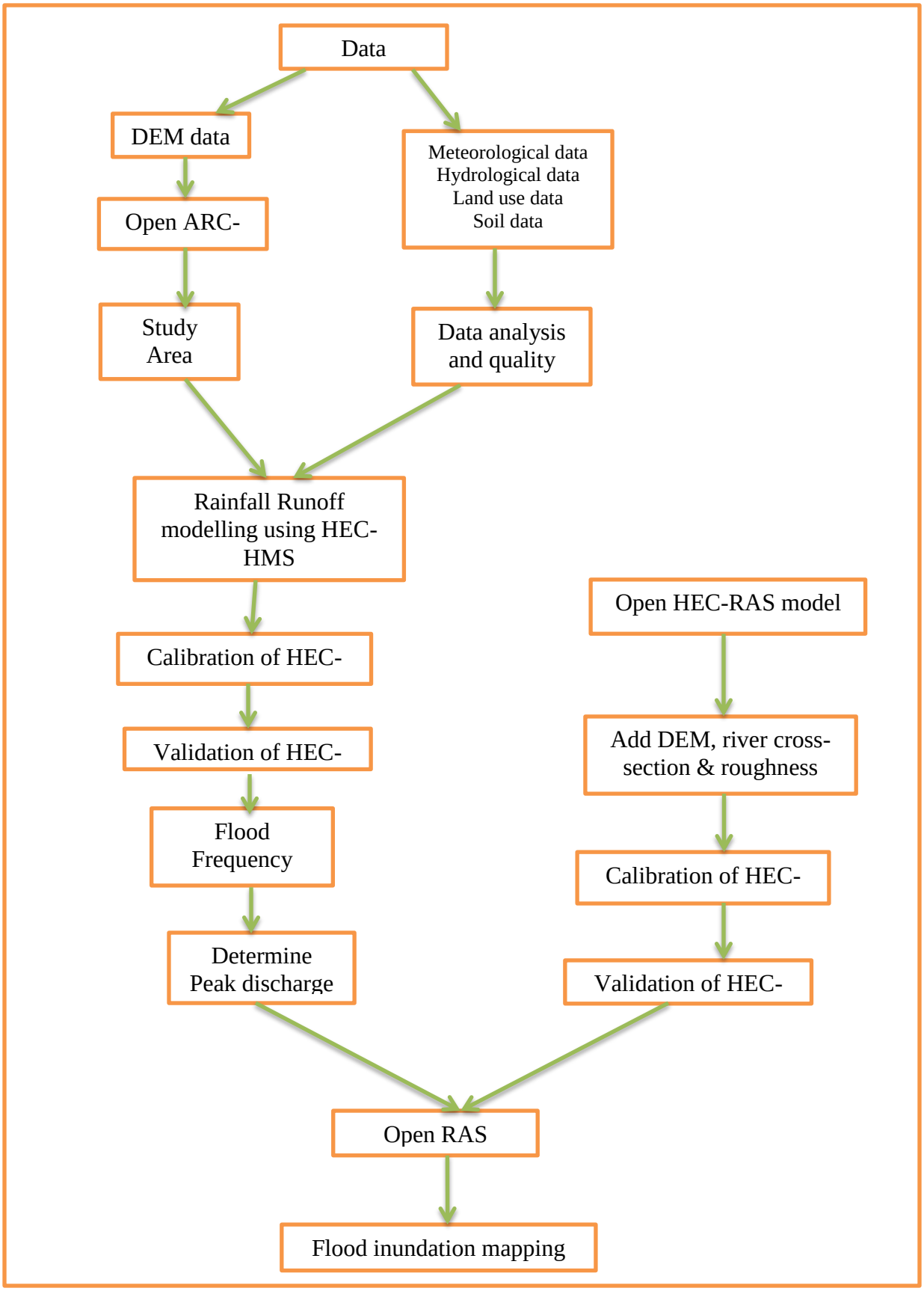

Figure 3.10: General frame work of the methodology for this specific study

3.5. DATA ANALYSIS

3.5.1 Meteorological data analysis

3.5.1.1 Filling of missing rainfall data

Due to shifting of the station or damage or fault of the rain gauge, there would be missed data during the recording period. So missed rainfall data have to be filled before using the data for both hydrological and hydraulic modeling. There are various methods to fill in missed rainfall data, like arithmetic mean, normal ratio, inverse distance, etc. To select the method used to fill in missed data, first the percentage of missed data has to be determined. If the percentage of missed opportunities is less than 10%, it is recommended to use the arithmetic mean method unless either the normal ratio or the inverse distance method can be used (Abdullah & Al-Ansari, 2022). For this study, the arithmetic mean method was used.

3.5.1.2 Testing for consistency of record

If the conditions relevant to the recording of a rain gauge station have undergone a significant change during the period of record, inconsistencies would arise in the rainfall data of that station (Hunziker et al., 2017) This inconsistency would be felt from the time the significant change took place. Some of the common causes of inconsistency of record are: (i) shifting of rain gauge stations to a new location; (ii) the neighborhood of the station undergoing a marked change; (iii) change in ecosystem due to calamities such as forest fires and landslides; and (iv) the occurrence of an observational error from a certain date. Checking for inconsistencies in a record is done by the double mass curve technique (Tabari et al., 2011).

The data on the annual or monthly rainfall of station X and also the average rainfall of the neighboring stations are arranged in reverse chronological order (i.e., the last record is the first entry and the oldest record is the last entry). The accumulated precipitation at station X (i.e.$\sum Px$) and the accumulated value of the average of the neighboring stations (i.e.$\sum Pav$) are calculated starting from last record. Values of $\sum Px$ are plotted along y-axis and $\sum Pav$ along X-axis (Subramanya, 2008).

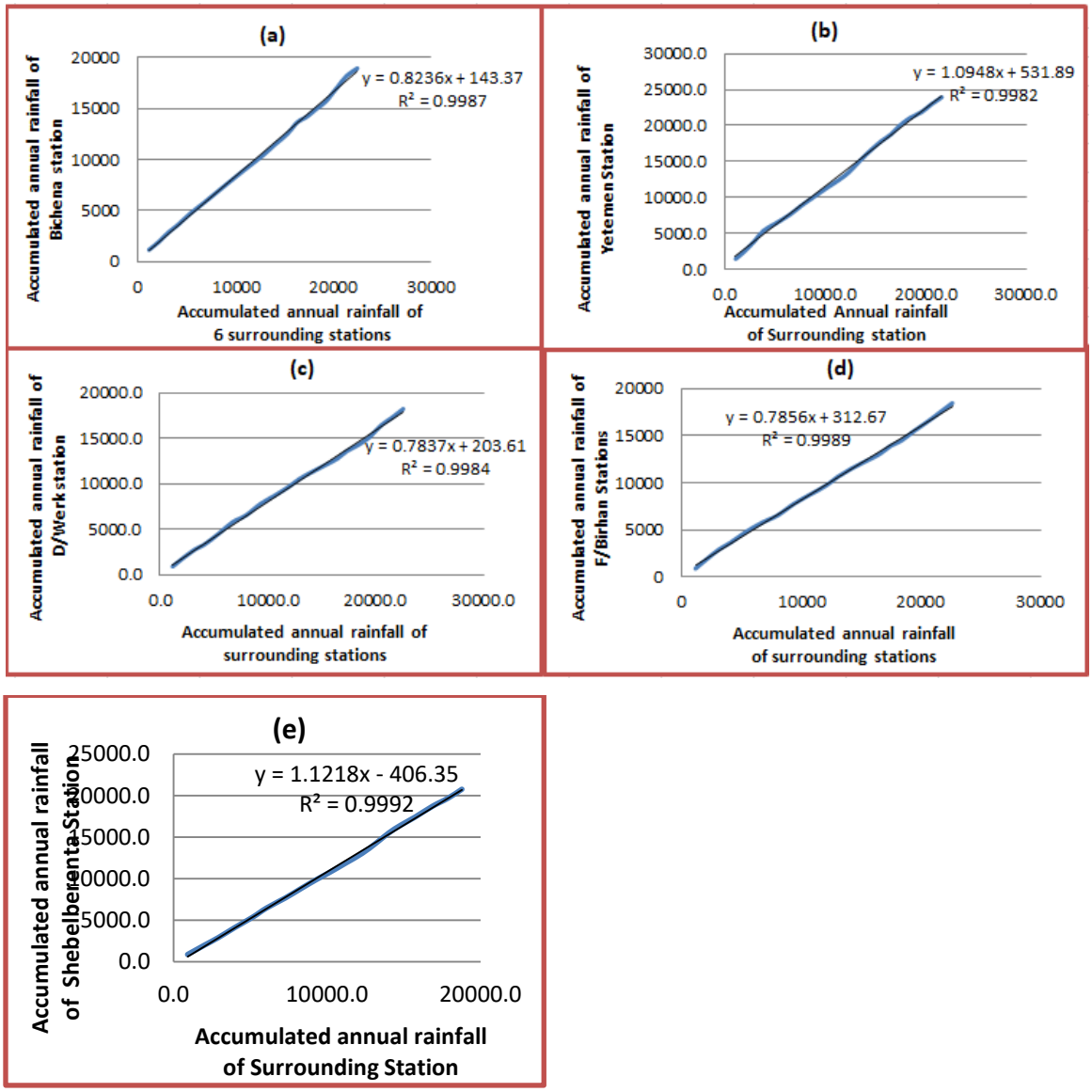

Figure 3.11: Double mass curve for different stations (a) Bichena (b) Yetemen (c) D/werk (d) F/birhan and (e) Shebelberenta Stations

As shown on Figure 4.1, the value of R^2 is approximately one and hence the data in all stations are consistent. Therefore, correction is not needed for all stations. The monthly rainfall data of the study area for year 1986 is shown in the Figure 4.2 and the maximum and minimum amount of rainfall occurs in June and December respectively.

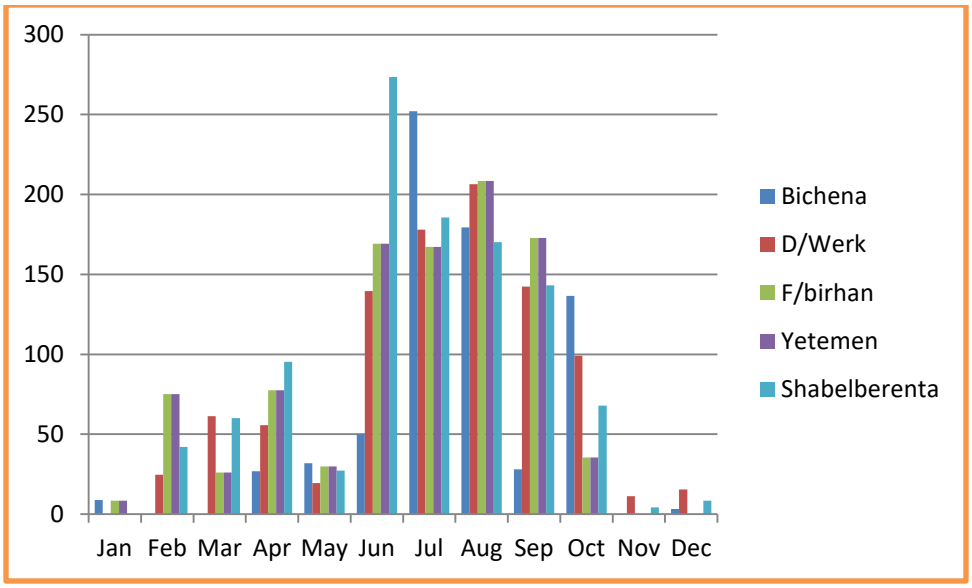

Figure 3.12: Monthly Rainfall of neighboring stations in 1986 (Refer Appendix C)

3.5.2 Stream flow data analysis

In this specific study area, the gauge station is located between Bichena and Yetemen towns under the Suha Bridge. For this specific study, nineteen years of daily stream flow data were obtained and collected from the Abay Basin Authority. The collected stream flow data had missing data, which was filled by Stata 13 software. The daily stream flow data after filling is shown in Figure. 4.3.

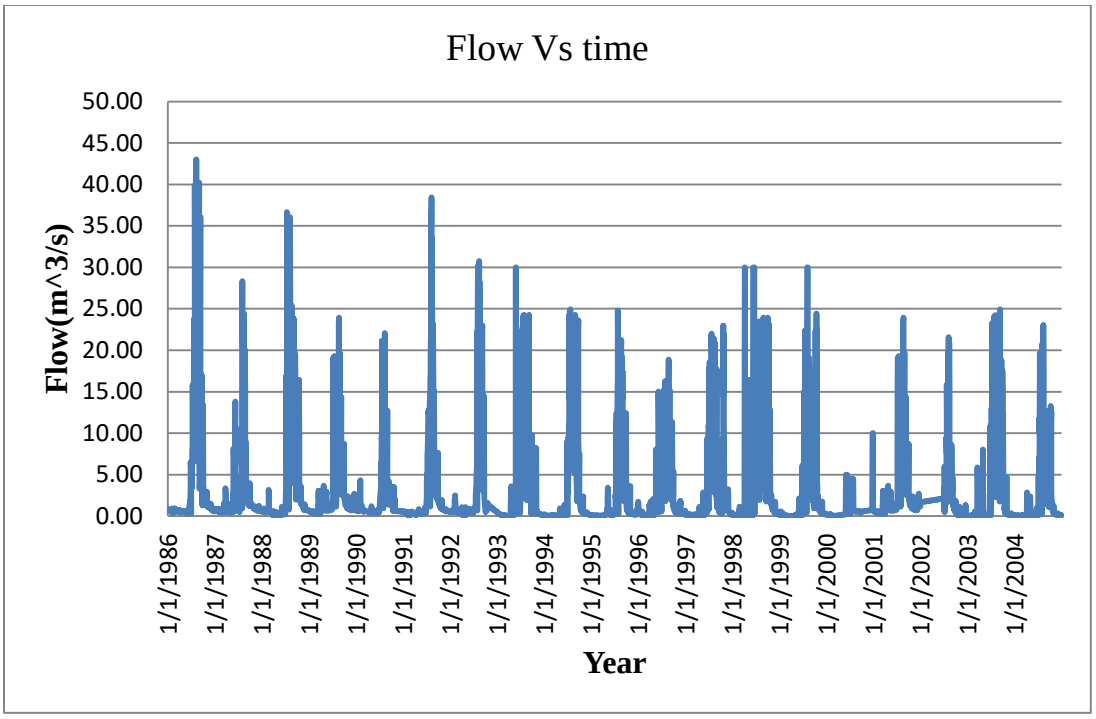

Figure 3.13: Daily stream flow data (01Jan1986- 31Dec2004) (Ref APPENDIX D)

3.6 HEC-HMS Model Analysis

3.6.1 Basin Model

The basin model represents the physical watershed. The user develops a basin model by adding and connecting hydrologic elements. Hydrologic elements use mathematical models to describe physical processes in the watershed. The hydrologic elements include sub-basins, reach, junction, source, sink, reservoir, and diversion. Under this, there are different tools that are used to perform different tasks: terrain reconditioning, preprocessing sinks, preprocessing drainage, identifying streams, and delineating elements (Rosegrant et al., 2000).

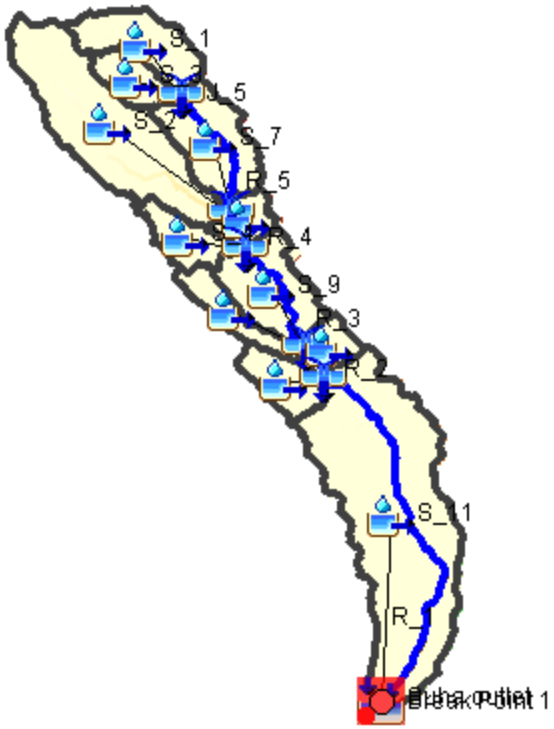

Figure 3.14: Junction, reach and sub-basins of the study area

a) Selecting Loss method

While a sub-basin element conceptually represents infiltration, surface runoff, and sub-surface processes interacting together, the actual infiltration calculation is performed by the loss method contained within the sub-basin. There are different types of loss methods: deficit and constant, exponential, green and amplified, gridding SCS curve number, SCS curve number method, etc. (Odyuo, 2020). All of the methods conserve mass. Most of the above methods have their own limitations and cannot be used directly without calibration. However, the SCS curve number method is the most recommended one, and used for this study. This method uses a composite curve number that represents all of the different soil groups and land use combinations in the sub-basins. This method assumes the sum of infiltration and precipitation left on the surface will always be equal to the total incoming precipitation (Thu et al., 2019).

i) Curve number determination

The two important data's used for curve number determination are land use/cover and Hydrologic soil group (HSG). The important soil characteristics that influence hydrological classification of soils are effective depth of soil, average clay content, infiltration characteristics and permeability (Scherrer & Naef, 2003). There are four hydrologic soil groups: Group A (low runoff potential), Group B(moderately low runoff potential), Group C(moderately high runoff potential), and Group D(high runoff potential) (Kumar et al., 2021). Based on this, the HSG of the study area are shown in the Table 4.1

Table 3.6 Soil type, Major LULC, hydrologic soil group and coverage area of each Sub-basins (Refer APPENDIX B1)

Sub-basins	Major Soil Type	MajorLC	HSG	Area(km^2)
1	Vertisols	Built Up Area	D	
	Luvisols	Cultivated Land	B	
	Lithosols	Forest Land	D	52.57
	Rendzians	Grass Land	D	
	Cambisols	Shrub and Bush Land	B	
2	Luvisols	Cultivated Land	B	
	Lithosols	Forest Land	D	154
	Rendzians	Grass Land	D	
3	Vertisols	Built Up Area	D	
	Luvisols	Cultivated Land	B	
	Lithosols	Forest Land	D	27.806
	Rendzians	Grass Land	D	

ii) Composite curve number

The curve number used in the simulation of hydrological modelling should be a composite curve number. Hence the curve number should represent the entire soil group and land use combinations in the sub basin (Sumarauw & Ohgushi, 2012).

It is calculated as follow:

$$Composite\ CN = \frac{\sum_{i=1}^{\infty}(\mathrm{CNi}*\mathrm{Ai})}{\sum_{i=1}^{\infty} Ai} \qquad \ldots\ldots\ldots\ldots\ldots\ldots\ldots\ 3.1$$

Where Ai = Subdivision area in each sub-basins

CNi = curve number of subdivisions in each sub-basins

Table 3.7 Composite curve number of each Sub-basin (Refer APPENDIX B2)

Sub basins	Major Soil Type	MajorLC	HSG	CNi	Ai	CN*Ai	Sum (CNi*A)	Sum (Ai)	Comp CN
1	Vertisols	Built Up Area	D	85	26.3	2234.2	4235.04	52.57	80.56
	Luvisols	Cultivated Land	B	75	5.3	394.27			
	Lithosols	Forest Land	D	77	10.5	809.57			
	Rendzians	Grass Land	D	80	4.2	336.44			
	Cambisols	Shrub and Bush Land	B	73	6.3	460.51			
2	Luvisols	Cultivated Land	B	75	77	5775	11842.6	154	76.9
	Lithosols	Forest Land	D	77	30.8	2371.6			
	Rendzians	Grass Land	D	80	46.2	3696			
3	Vertisols	Built Up Area	D	85	2.3	189.1	2156.08	27.80	77.54
	Luvisols	Cultivated Land	B	75	13.9	1042.7			
	Lithosols	Forest Land	D	77	3.3	256.9			
	Rendzians	Grass Land	D	80	8.3	667.34			

iii) Initial abstraction

It is a parameter that accounts for all losses prior to runoff and consists mainly of interception, infiltration, evaporation, and surface depression storage. In theory all rainfall minus initial abstraction will generate the runoff from the specified catchment. it is a function of maximum retention and calculated as follow (Porter & McMahon, 1971).

$$Ia = 0.2S, \qquad \text{…….. 3.2}$$

$$S = \frac{25400}{CN} + 254 \qquad \text{..... 3.3}$$

Where, Ia = initial abstraction S = maximum storage and CN = composit curve number

Table 3.8 Maximum retention and initial abstraction of each subbasins (Refer APPENDIX B3)

Sub basins	Major Soil Type	MajorLC	HSG	CNi	Comp CN	S	Ia
1	Vertisols	Built Up Area	D	85			
	Luvisols	Cultivated Land	B	75			
	Lithosols	Forest Land	D	77	80.56	569.3	113.9
	Rendzians	Grass Land	D	80			
	Cambisols	Shrub and Bush Land	B	73			
2	Luvisols	Cultivated Land	B	75			
	Lithosols	Forest Land	D	77	76.9	584.3	116.86
	Rendzians	Grass Land	D	80			
3	Vertisols	Built Up Area	D	85			
	Luvisols	Cultivated Land	B	75	77.54	581.57	116.31
	Lithosols	Forest Land	D	77			
	Rendzians	Grass Land	D	80			

IV) Imperviousness (%)

Impervious surface are areas covered with roads parking lots, roofs and other surfaces that do not allow water to soak in to the ground.it depend on the land use land cover of the area. The result is a significant increase in the volume of storm water that runs off the land and significant impact to local water way (Raspati et al., 2017). Almost all part of the watershed is agricultural land and open space (grass, pasture) except some part of Bichena city. Some part of Bichena city is included in the watershed. So the watershed includes agricultural area, grass & pasture land. Therefore by considering the above land use type and referring Table 4.4, the imperviousness of the study area was 3.5%.

Table 3.9 Imperviousness of different land uses

Land use	% impervious area
Industrial	90
Commercial	95
High density residential(15 homes/acre)	60
Medium density residential(5 homes/acre)	30
Low density residential(2homes/acre)	15
Agricultural	5
Open space(parks, grass, pasture)	2

Source: Wisconsin Department of Transportation (2012)

Table 3.10 Calculated loss determination parameters (Refer APPENDIX B4)

Sub-basins	Parameters	unit	Value
1	Area (A)	km^2	52.57
	Curve number (CN)		80.58
	Initial abstraction (Ia)	mm	113.86
	Imperviousness	%	5
2	Area (A)	km^2	154
	Curve number (CN)		76.9
	Initial abstraction (Ia)	mm	116.86
	Imperviousness	%	5
3	Area (A)	km^2	27.81
	Curve number (CN)		77.54
	Initial abstraction (Ia)	mm	116.31
	Imperviousness	%	5

b) Selecting transform method

While a sub-basin element conceptually represents infiltration, surface runoff, and sub-surface processes interacting together, the actual surface runoff calculations are performed by a transform method contained within the sub-basin. A total of nine different transform methods are provided. The choices include SCS unit hydrograph methods, Snyder unit hydrograph a kinetic wave implementation, a linear quasi-distribute method, etc. The most commonly used method is SCS unit hydrograph method and was used for this study (Thu et al., 2019).

c) Selecting a base flow methods

While a sub-basin element conceptually represents infiltration, surface runoff, and sub-surface processes interacting together, the actual subsurface calculations are performed by a base flow method contained within the sub-basin. A total of six different base flow methods like linear reservoir base flow, constant monthly base flow, bounded recession base flow, recession base flow and others are provided. For this study base flow methods was not used because the river is not perennial rather it is intermittent (Thu et al., 2019).

d) Selecting a reach routing method

While a reach element conceptually represents a segment of stream of river, the actual calculation is performed by a routing method contained within the reach. Different routing methods are provided. Each of the methods implements a hydrologic routing methodology as compared to a hydraulic approach that implements the full unsteady flow equation. Each method include in the program provides a different level of detail and not all method are equally adopt at representing particular stream. For this study, Muskingum routing method was used. The Muskingum X is the weighting between inflow and outflow and it ranges from 0.0 to 0.5 (Retsinis et al., 2020).

3.6.2 Meteorological Model

Meteorological models are one of the main components in project. The principal purpose is to prepare meteorological boundary condition for sub-basins. Consequently, it is must to create at least one basin model before creating meteorological model. The meteorological model calculates the precipitation input required by sub basin element. It can be used with many different basin models (Collischonn et al., 2008).

However, results computed by meteorological model will be matched with the sub-basins in the basin model using the name of the sub-basins. If sub-basins in different basin model have the same name, they will both receive the same boundary conditions from the meteorological model. Careful naming of sub-basins is necessary so that the correct boundary condition is computed for each one (Lehner & Grill, 2013).

3.6.3 Control Specification

The Control Specifications is defined as the time related information in the simulation, including the starting dates, ending dates, and the computational time interval. The function of control specifications is to set the starting and ending dates and times and time (computation) intervals. The time step for HEC-HMS model calibration for the catchment is divided into different time steps as for calibration, simulation, and validation (Van Chinh et al., 2013).

The time is divided into two sections and used data spanning 19 years, beginning on January 1, 1986, and ending on December 31, 2004. The first one is used for calibration and spans the period from January 1, 1986 to December 31, 1998. The second one runs from January 1, 1999 to December 31, 2004, and is for validation.

3.6.4 Time series

It is another HEC HMS model component. Time series data inserted in this component are precipitation data and discharge data. These data used for calibration and validation purpose. First starting and ending date and time was inserted in the time window and after that both the precipitation and discharge data were inserted manually in their specified table space (Halwatura & Najim, 2013).

3.7 Calibration and Validation of HEC-HMS Model

3.7.1 Calibration

Model calibration is a systematic process of adjusting model parameter values until model results match with the observed data (Hanson et al., 1999).

There are different parameters that are adjusted until the observed and simulated flow closes each other. These parameters are curve number, lag time, initial abstraction. The quantitative measure of the match is described by the performance indicators like Nash Sutcliff efficiency, root mean square error, percent of bias. In the rainfall-runoff models, this performance indicator measures the degree of variation between computed and observed hydrographs (Moriasi et al., 2007). Different literatures recommend using 70 % of the total data for calibration purpose and the remaining 30% for validation. Accordingly, a total of nineteen years of daily stream flow data were used for this

investigation, of which thirteen years' worth were used for calibration and the remaining six years' worth were used for validation. For calibration purpose the data starts from 01Jan1986 and ends at 31Dec1998.

3.7.2 Validation

Validation of Hydrological models deliver an assessment of the model's capability to accurately reproduce well-known results (Biondi et al., 2012). This is performed by running the model with the calibrated curve number, lag time and initial abstraction obtained in the calibration process. It is simply used to rechecking of the result of computed and simulated peak discharge by using another stream flow data which is not included in calibration process. For validation purpose, six years stream flow data starting from 01 Jan 1999 up to 31 Dec 2004 was used.

3.8 Performance of HEC HMS Model

Before using HEC HMS model for further analysis purpose such as for flood frequency analysis, first it's performance have to be checked. There are different performance indicators of this model. These are Nash Sutcliff efficiency (NSE), root mean square error (RMSE), and percent of bias (PBIAS) (Moriasi et al., 2015; Fanta & Sime, 2022).

a) Nash Sutcliff efficiency (NSE)

This indicates a correlation of computed value and agreement of the mean. Its value ranges from 0 to 1. NSE =0, computed value not matched with observed value and NSE = 1, the model value perfectly matched with observed value.

$$NSE = 1 - (\sum_{i=1}^{n}(qoi - qsi) \,/\, \sum_{i=1}^{n}(qoi - qsa)) \qquad \text{.....3.4}$$

b) Root mean square error (RMSE)

It measures the average difference between values predicted by a model and the actual values. It provides an estimation of how well the model is able to predict the target value. The lower value of RMSE indicates better model performance and higher value shows the model result not matched with that of observed one.

$$RMSE = \frac{\left(\sqrt{\sum_{1}^{n}(Yobs - Ysim)^2]}\right)}{\sqrt{\sum_{1}^{n}(Yobs - YaveSim)^2}} \qquad \text{..... 3.5}$$

c) Percent of bias (PBIAS)

It measures the average tendency of simulated value to be larger or smaller than observed value. The optimal value is 0. Positive value present model underestimation bias and negative value presents model overestimation bias.

$$PBIAS = \frac{\sum_1^n (YiObs - YiSim)}{\sum_1^n YiObs} \quad \text{…….. 3.6}$$

Table 3.11 Model performance indicators.

Performance ratings	NSE	RMSE	PBIAS
Very good	0.65<NSE<=1	0<RMSE <=0.6	PBIAS < ±15
Good	0.55<NSE<=0.65	0.6<RMSE <=0.7	±15<=PBIAS < ±20
Satisfactory	0.4<NSE<=0.55	0.7<RMSE <=0.8	±20<=PBIAS < ±30
Unsatisfactory	NSE<=0.4	RMSE >0.8	PBIAS >= ±30

3.9 Flood Frequency Analysis

Hydrologic processes such as floods are exceedingly complex natural events. They are the resultants of a number of component parameters and are therefore difficult to model analytically. For example, the flood in a catchment depends on the characteristics of the catchment, including rainfall and antecedent moisture conditions; each of these factors in turn depends upon a host of constituent parameters. This makes the estimation of the flood peak a very complex problem, leading to many different approaches. One of these is the statistical method of frequency analysis. The most commonly used distribution functions are: Gumbel's extreme-value distribution, log-Pearson type III distribution, and log normal distribution (Cunnane, 1988). HEC-HMS model was selected for flood frequency analysis. The above methods are used only to compare the values obtained from HEC HMS and to know the difference in flood magnitude between HEC HMS models. The analysis is performed at a 2 year, 5 year, 10 year, 25 year, 50 year, and 100 year return periods.

3.10 HEC RAS Model Analysis

This model requires data like river cross section data, stream flow data (flood hydrograph), terrain data, and Manning's roughness coefficient. The river cross section data may be collected from a field survey using GPS or a total station or directly from the terrain data (DEM) by digitizing it. For this thesis work, river cross-section data was collected from the field.

In HEC-RAS simulation, the required parameters that should be adjusted in order to run the model is roughness coefficient of the river channel and flood plain. Basically, after giving the project name, the plan data, the geometric data, and the flow data are required to run the model and obtain results from the model. The plan data comprises information that is related to the model specifications for the description of the flow regime, Geometric data comprises the size, shape, and connectivity of the stream cross-sections, and flow data contains the flow rate for different return periods. The SI unit system also should be adjusted unless errors may occur. For this study, the international system (metric system) was used.

a) Importing geometric data & adding flow data

Geometric data was collected from the field using a total station and imported to HEC-RAS for further analysis. After the cross-section data added, the flow data as an upstream boundary condition was inserted. The computation time was inserted based on the starting and ending dates of the stream flow data. This stream flow data was obtained from the HEC HMS model result.

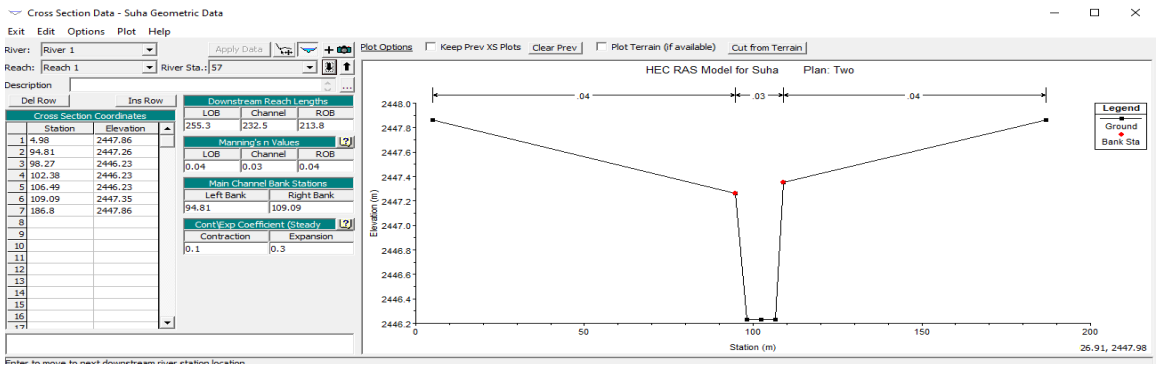

Figure 3.15: Sample cross section data profile at station 57 in HEC RAS window

b) Manning roughness coefficient

The roughness coefficient incorporates many factors that contribute to the loss of energy in a stream channel. The major factors are channel-surface roughness, which is determined by the size, shape, and distribution of the grains of material that line the bed and sides of the channel (the wetted perimeter). Five other main factors are channel-surface irregularity, channel shape variation, obstructions, type and density of vegetation, and degree of meandering (Cowan, 1956). By relating the Suha river channel and flood plain characteristics with the Table 4.6, it was assigned 0.04 for the main channel and 0.06 for the flood plain.

Table 3.12 Channel description and roughness coefficient (Chow, 1959)

types of channel and description	roughness coefficient		
	min	normal	max
A. minor streams			
1.stream on plains:			
a. clean, straight, full stage, no rift or deep pools	0.025	0.03	0.033
b. same as above, but more stones and weeds	0		
c. clean, winding, some pools and shoals	0.03	0.035	0.04
d. same as above, but some weeds and stones	0.033	0.04	0.045
e. same as above, lower stages more ineffective slopes and sections	0.04	0.048	0.055
f. same as typed, but more stones	0.045	0.05	0.06
g. sluggish reaches, weedy, deep pool			
2.mountain stream, no vegetation in channel, banks usually steep, trees and brushes along banks			
a. bottom: gravel, cobbles, and few boulders	0.03	0.04	0.05
b. bottom: cobbles and large boulders	0.04	0.05	0.07
B. major stream			
1.regular sections with no boulder	0.025		0.06
2.irregular and rough section	0.035		0.1

c) Boundary condition

There are four types of boundary conditions that can be applied to the outer boundary of a flow area. These boundary condition types are: flow hydrograph, stage hydrograph, normal depth, and rating curve (Pappenberger et al., 2006). External boundary condition locations can be added to the geometry either in RAS Mapper or in the geometric data

editor. Flood hydrographs for upstream boundary conditions and normal depths for downstream boundary conditions was used.

3.11 Unsteady Flow Analysis

The unsteady flow computational program in HEC-RAS uses the same hydraulic calculations (cross-section properties) that HEC developed for steady flow. The user is required to enter boundary conditions at the entire external boundary of the system as well as any desired internal locations. For the hydraulic model HEC RAS, in the case of unsteady flow, it is necessary to adjust the simulation starting and ending dates with the start and ending times of the simulation. So that the simulation time window for the different return periods is fixed from January 1, 1986, to December 31, 1986, for the start and end of the unsteady flow simulation.

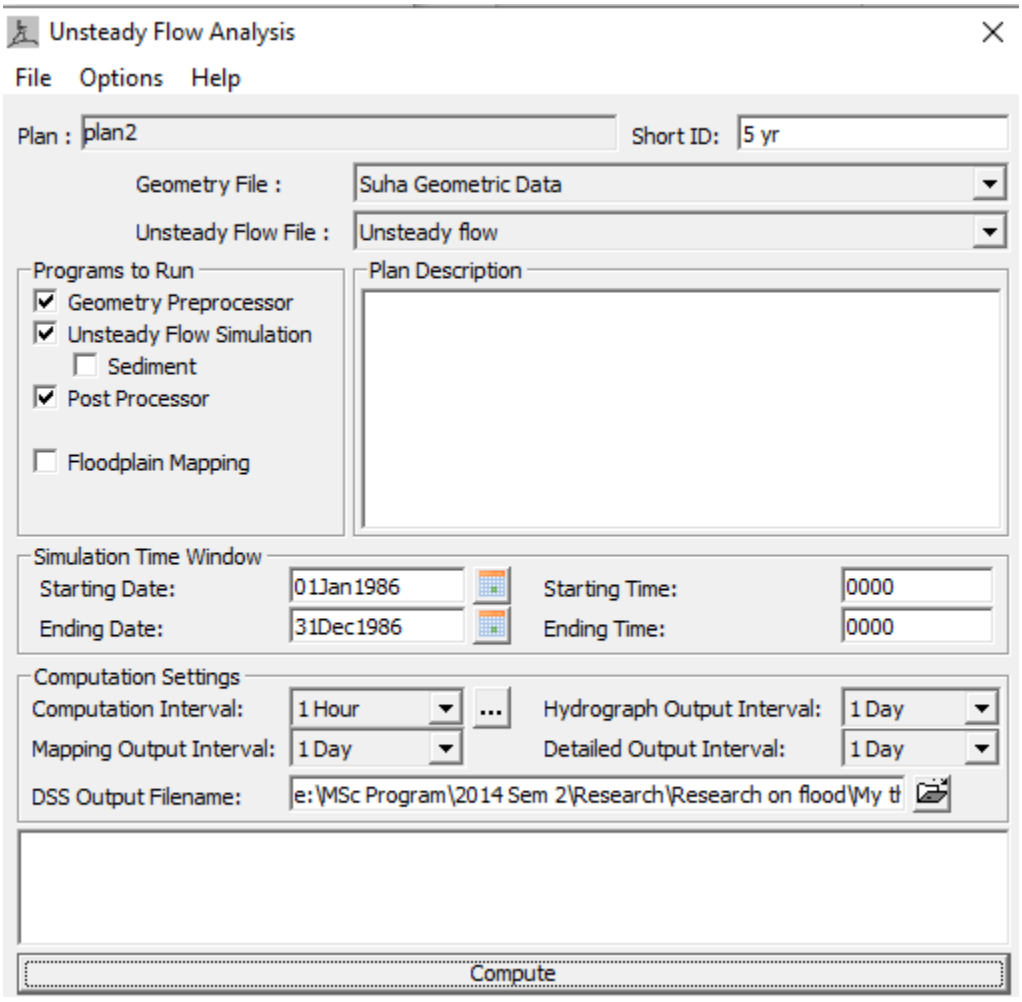

Figure 3.16: Unsteady flow analysis time window adjusted to run

3.12 Calibration and Validation of HEC RAS Model

HEC RAS model calibration and validation can be done qualitatively or quantitatively. Qualitatively means using a satellite image of the intended study area and then comparing it with a simulated one. On the other hand, quantitatively, it is possible to calibrate and validate using observed water levels. But for this specific study, satellite images were used for comparison due to a lack of observed water level data. The satellite images were downloaded from Landsat 7 for a different period and then computed the normalized difference water index (NDWI) to get the required image using the following formula.

NDWI = (Band 4 – Band 5) / (Band 4 + Band 5) …….. 3.7

a) Calibration

Calibration is the process of varying the parameters or coefficients of a hydrologic method so that it can estimate simulated water levels and flood maps consistent with local observed water levels and flood-inundated maps. Hydraulic parameters that are varied include roughness coefficients and expansion and contraction coefficients. The HEC-RAS model is calibrated against Manning's roughness coefficient (n-value) using satellite image extracted from Landsat 7 on October 1, 1998.

b) Validation

Model validation provides an assessment of the model's ability to accurately reproduce known results. This is performed by running the model with the calibrated n values. The computed flood inundated map is compared to the satellite image. For this specific study, the satellite image extracted from Landsat 7 on October 15, 2004 was used to validate the model.

4. RESULTS AND DISCUSSION

4.1 Calibration and Validation of HEC HMS Model

HEC HMS model calibration and validation are very essential before proceeding to further analysis, such as flood frequency analysis of different return periods. The adjusted parameters were curve number, initial abstraction, and lag time. These parameters have to be adjusted until a good correlation between the observed and simulated flows can be obtained. To say a good correlation is obtained between observed and simulated flow, the model performance parameters such as Nash-Sutcliffe Efficiency, root mean square error, and percent of bias have to be in the optimum range.

The HEC-HMS model calibration result shows that the values of NSE, PBIAS, and RMSE were 0.723, 10.83%, and 0.57 respectively. According to Moriasi et al., (2015), NSE values of 0.65 to 1 indicate that the model performs extremely well, values of 0.55–0.65 show that the model performs good, and the NSE value below 0.4 shows unsatisfactory. According to Fanta & Sime, (2022), the PBIAS value should be lower than (± 15%) and RMSE value should be 0-0.6 to say the model calibration is very good. The simulated and observed peak discharges were 39.4 and 43.0 m3/s, respectively. This indicates that the peak discharge was slightly under-predicted during model calibration. But the statistical metric values obtained during model calibration were under very good level of accuracy. Different literatures accept up to 30% difference between simulated and observed result (Manandhar, 2010). Therefore, the HEC-HMS model well simulated the Suha watershed runoff during the calibration phase. The detailed calibration result of the year from January 1, 1986, to December 31, 1998, and the flood hydrograph are shown in Figures 4.1 and 4.2, respectively.

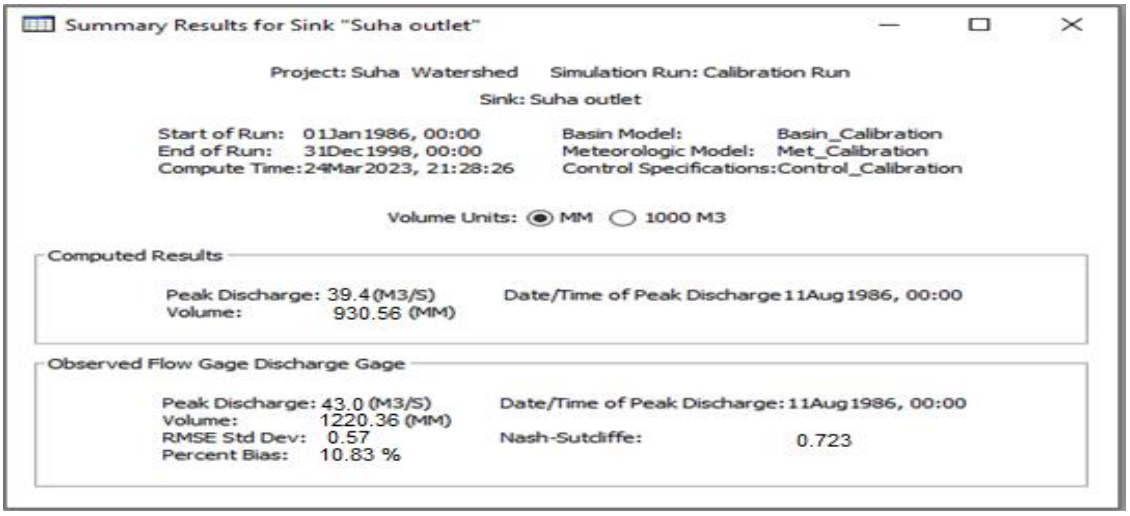

Figure 4.1: Result of HEC HMS model calibration

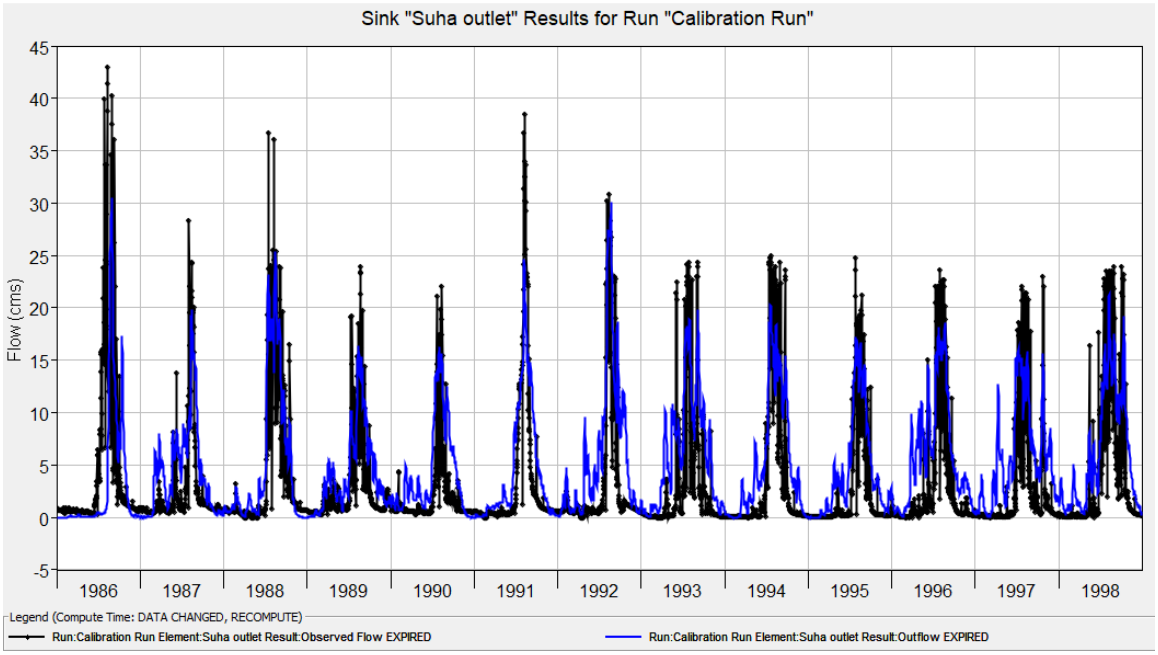

Figure 4.2: Simulated and observed flow graphical result for calibration

Figure 4.2 shows the observed and simulated streamflow during HEC-HMS calibration. At some year, such as 1986, 1988, and 199, the observed peak runoff is above the simulated hydrograph. Sometimes runoff reach at peak level for very short time and return to the normal level and this condition make the result not fit to the model simulation. However, the statistical parameters show better performance of the model.

The HEC-HMS model validation is performed by using the calibrated curve number and roughness coefficient for the years 01 January 1999 to 31 December 2004. The HEC-HMS model validation result shows that the values of NSE, PBIAS, and RMSE were 0.753, 8.253%, and 0.485, respectively. The simulated and observed peak discharges were 40.9 and 40.0 m^3/s, respectively. This indicates that the simulated peak discharge close to observed discharge during model validation. The result of performance indicators obtained during model validation was under very good level of accuracy. Therefore, the HEC-HMS model well simulated the Suha watershed runoff during the validation phase. The detailed validation result of the year from January 1, 1999, to December 31, 2004, and the flood hydrograph are shown in Figures 4.3 and 4.4, respectively.

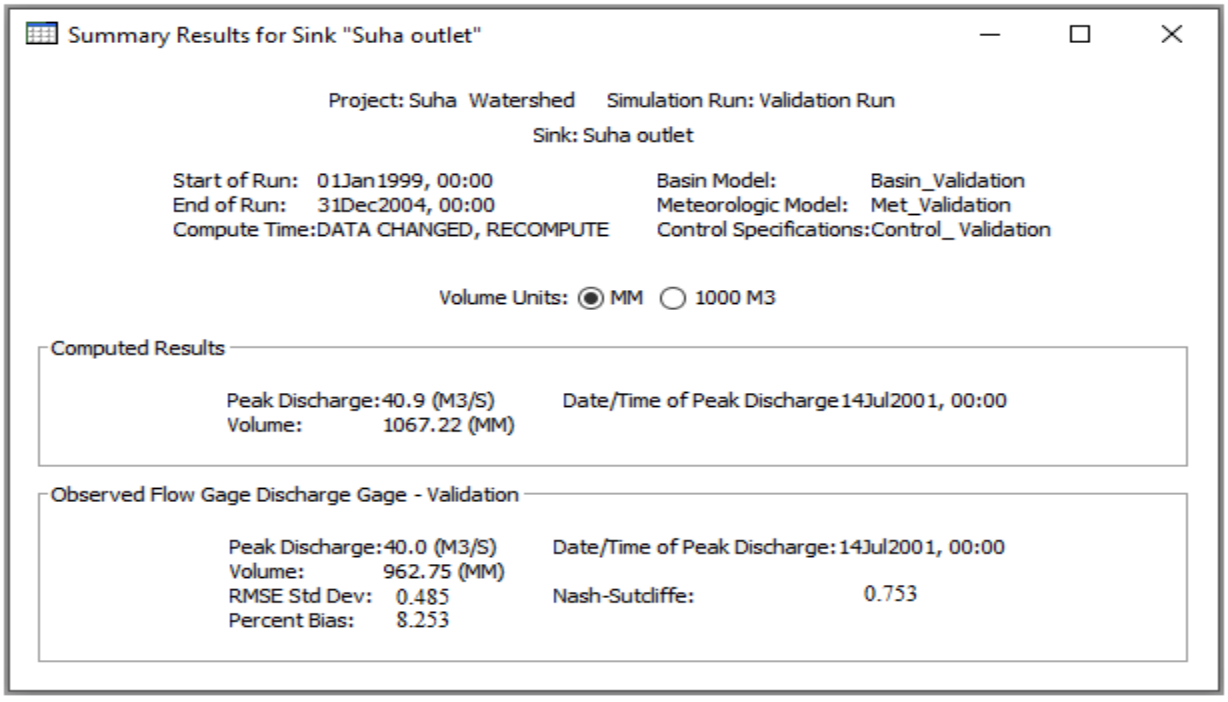

Figure 4.3: Validation result of HEC HMS model

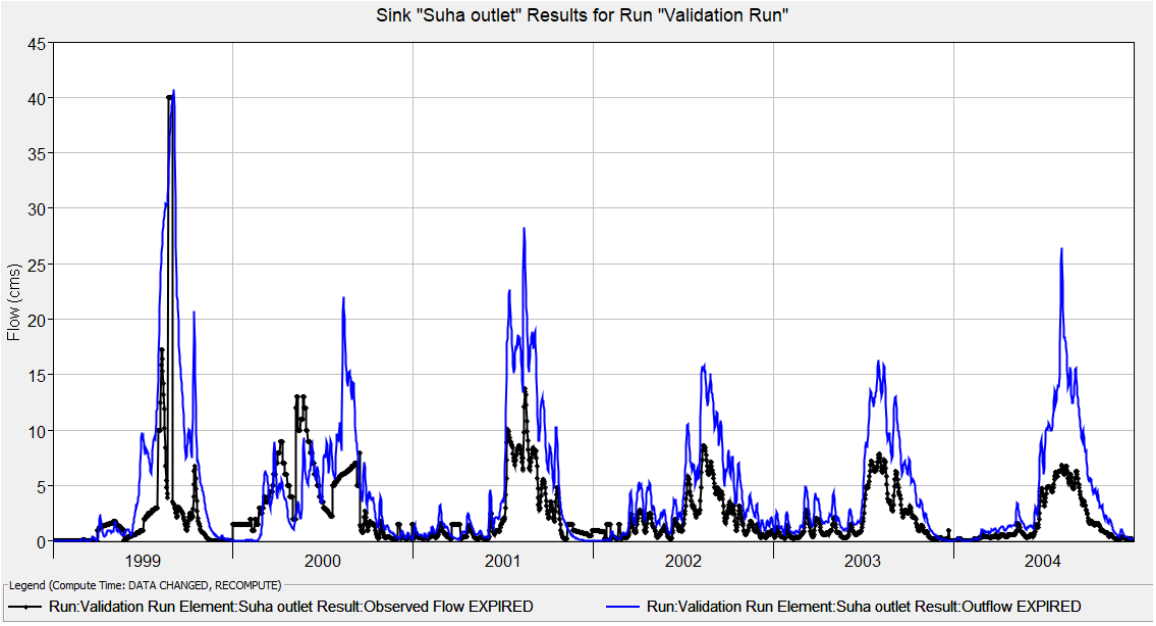

Figure 4.4: Simulated and observed flow graphical result for validation

It is observed that there is a 5.31% increment in NSE value in the model validation relative to the model calibration. This indicates the model value perfectly matched with observed value in case of validation than calibration. However, there was a 19.32 and 11.82% reduction in PBIAS and RMSE, respectively, in the model validation. The reduction of this two parameters shows better model performance since the lower value of both RMSE and PBIAS indicates better model performance and higher value shows the model result not matched with that of observed one.

The performance indicators are within the ideal range. The stream flow as predicted and as observed is very similar. As a result, we may utilize the HEC-HMS model to determine peak discharge at various return periods. For the purpose of preparing a flood inundation maps on the HEC-RAS, these peak discharges at various return periods will be used as inputs.

The performance of HEC-HMS model is evaluated with calibration and validation. To evaluate the performance of this model, three performance indicators were used. These indicators were NSE, PBIAS, and RMSE and their results obtained during calibration and validation processes were very good. This implies the model has good performance and now it can be used for flood frequency analysis.

4.2 Flood frequency results for different return periods

There are different techniques to forecast flood frequency at different return periods. These may be done by using manual calculations using the Gumbel distribution, log normal, and log-Pearson Type III methods, or by using the HEC HMS Model. Depending on antecedent soil moisture conditions and other hydrologic parameters, there may not be a direct relationship between rainfall and flood frequency (Sahoo & Ghose, 2021). Therefore, the HEC HMS model is better suited to perform flood frequency analysis by using a frequency storm of 24 hour duration. The rainfall depth was obtained from the IDF curve of the surrounding stations. In this specific study, Gumbel distribution and Log-Pearson Type III were used as techniques for flood frequency analysis. But these analysis techniques were used only to compare with the HEC HMS model flood result values, as shown in Table 4.1. The above-mentioned flood frequency analysis techniques are used only to know the difference in flood magnitude from the HEC HMS model result, and the HEC HMS model result were used for simulation of flood mapping using the HEC RAS model.

Table 4.1 Peak flood result comparison at different return period of the outlet

frequency analysis methods			
Return period	Gumbel distribution	Log pearson type III	HEC HMS
2	38.24	35.33	50.4
5	50.12	45.36	76.1
10	70.4	89.33	107
25	95.85	110.65	151.9
50	120.68	159.45	211
100	168.67	201.23	301

From Table 4.1, the HEC-HMS results at different return period are greater than the other two methods, Gumbel distribution and Log Pearson type III methods. Both Gumbel distribution and Log Pearson type III methods uses annual rainfall to calculate the runoff. But the HEC-HMS model consider different parameters to determine the peak flood. HEC-HMS model uses rainfall, curve number, initial abstraction, lag time and imperviousness of the area to calculate the flood. These parameters have a considerable

impact on flood. Therefore, the result obtained from HEC-HMS model is more accurate and acceptable than other methods.

4.3 Calibration and validation of HEC RAS model

Before using HEC-RAS model for preparation of flood inundation mapping, first its performance was to be checked. To do that, satellite image used as observed data. To say the model has good performance, the satellite image and the map done on HEC-RAS have to be similar. If the two maps do not similar, another trial is conducted by changing the roughness coefficient. For calibration and validation of this model, past observed flooded areas were downloaded from Landsat 7 for two consecutive times, one for calibration and the other for validation. For this study, even if there was enough observed data from satellite imagery, its resolution was lower. Therefore, two time spans of flood events (October 1, 1998, and October 15, 2004) were downloaded and relatively have good resolution for further analysis of the normalized difference water index (NDWI) to compare with the flood inundation map obtained from model simulation. The calibration and validation of the HEC RAS model were obtained accordingly. As shown in Tables 4.2, the initial Manning roughness that was obtained from Cowan (1956) has been substituted with the value from the calibration of the HEC RAS model through trial and error steps. Therefore, for this study, the calibrated value of the right bank and left bank obtained was 0.04 and the main channel was 0.03.

Both the calibration and validation were done until the two maps, the satellite image and map done on HEC-RAS, become similar. This is done by changing the roughness coefficient that is used in HEC-RAS during flood inundation map. Once the two maps becomes similar (i.e. the map from Landsat 7 and the map done on HEC-RAS), the model has good performance.

Table 4.2 Initial and calibrated manning's roughness coefficient

Parameter	Initial n	Calibrated n
Left bank	0.06	0.04
Main channel	0.04	0.03
Right bank	0.06	0.04

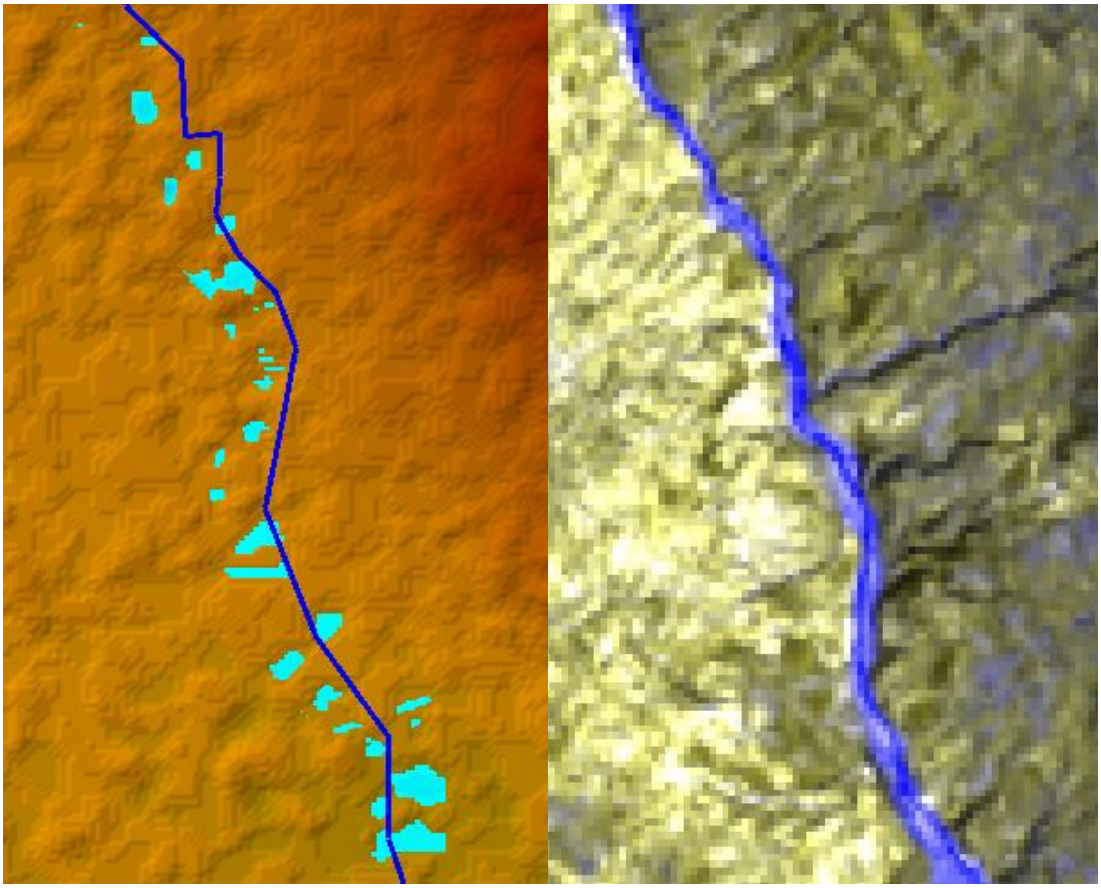

(a) (b)

Figure 4.5: Calibration of HEC RAS model for 01Oct1998 (a) simulated image (b) observed image

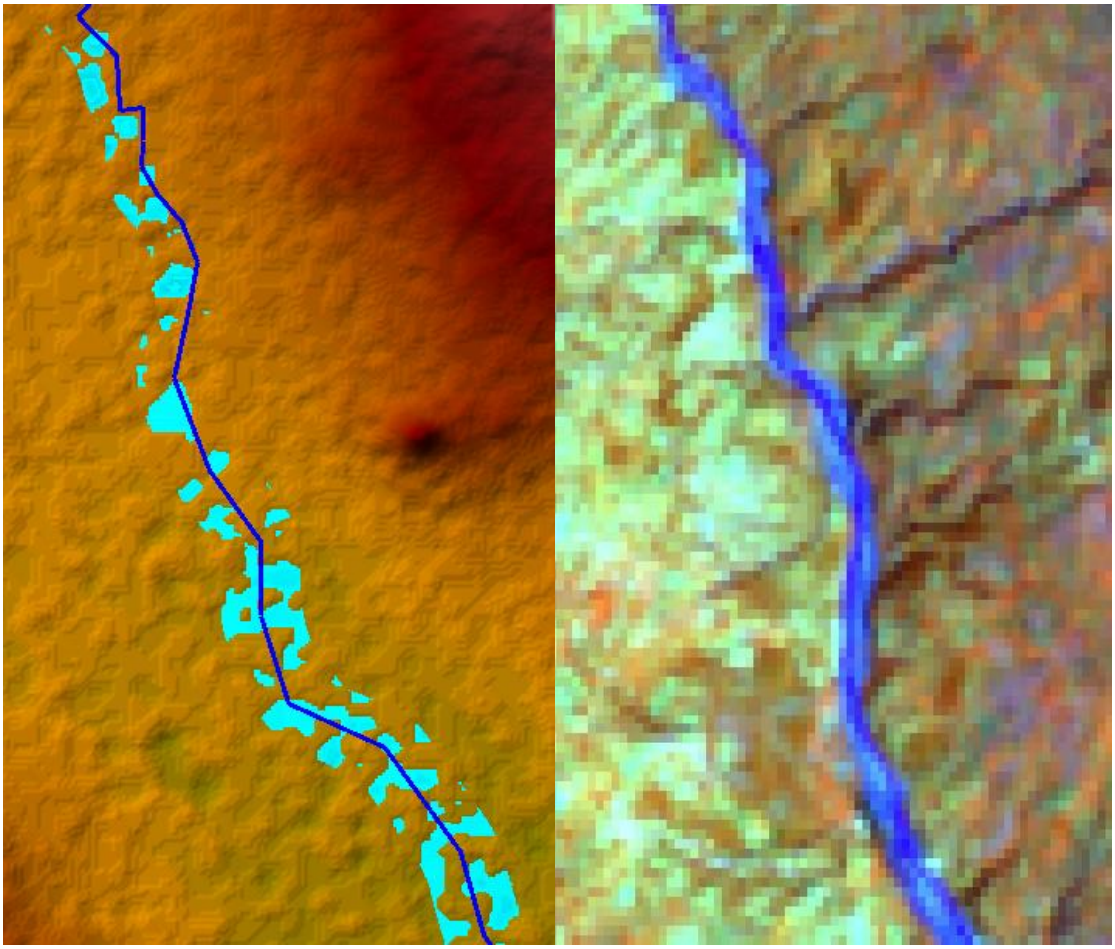

(a) (b)

Figure 4.6: Validation of HEC-RAS model for 15Oct2004 (a) simulated image (b) observed satellite image

The simulated image was obtained from RAS mapper using the calibrated roughness coefficient and stream flow data from HEC-HMS model at year 2004. As the calibration and validation result shows, the satellite image and the map done on the HEC-RAS model are similar. This implies that the model has good performance and now the model can be used to do flood inundation mapping.

4.4 Flood Inundation Mapping

Flood-inundated mapping is an important mechanism for river flood assessment in a hydraulic simulation. These forecasts of flood areas for different return periods have a vital role in making a prevention technique before the flood occurs. For this specific study in HEC RAS simulation, the flood-inundated map was determined using the RAS

mapper. For different return periods, the flood-inundated area was determined, and are shown in the Figure 4.7. As shown in the Figure 4.7 for the 2-year return period, only some stations was flooded. However, at 50yr and 100yr return period all station are fully flooded.

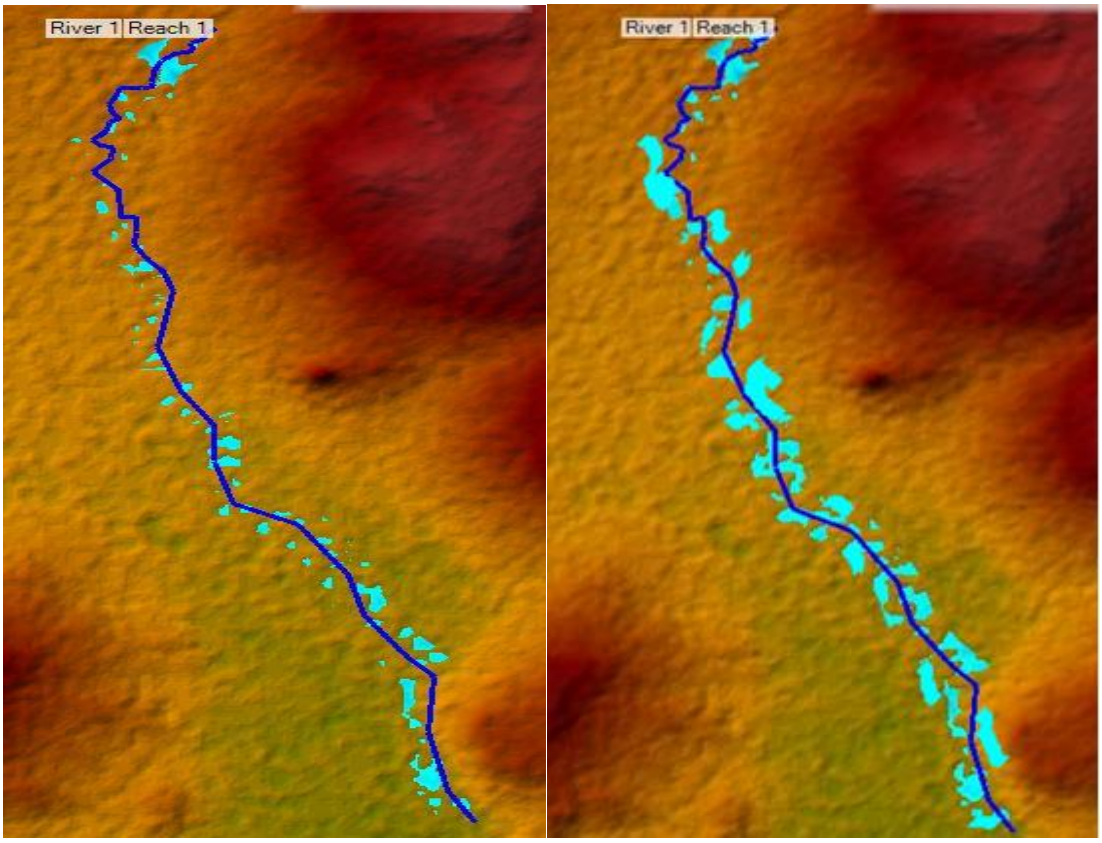

(a) (b)

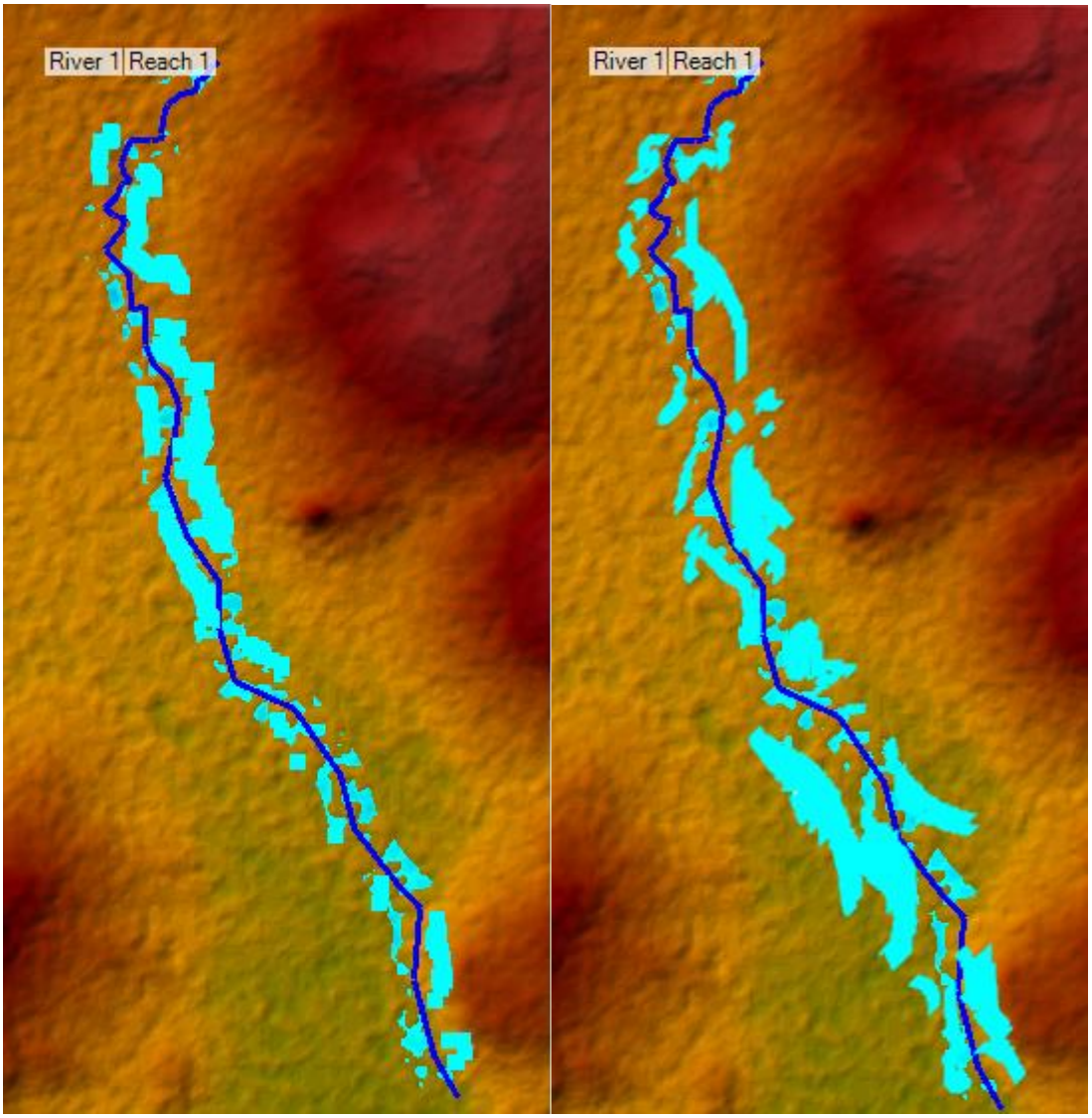

(c) (d)

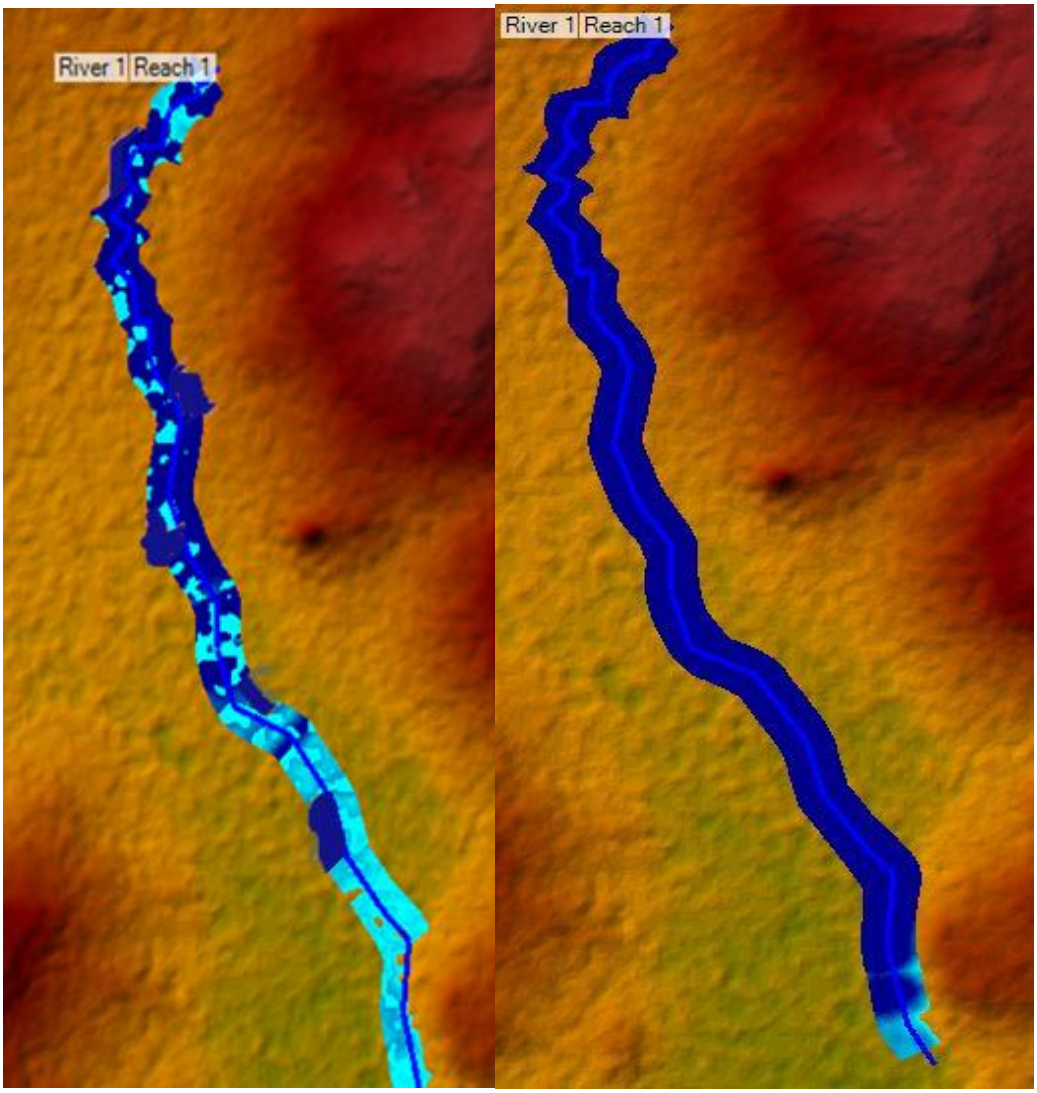

(e) (f)

Figure 4.7: Flood inundated map for different return periods (a) 2yr RP (b) 5yr RP (c) 10yr RP (d) 25yr RP (e) 50yr RP and (f) 100yr RP

For further analysis such as for determining the risk of the flood for different return periods, it is mandatory to calculate flood inundated area. Therefore after the analysis of the entire flood inundated maps the inundated area for the different return periods determined and shown in Table 4.3.

Table 4.3 Flood inundated areas for different return periods

RP		2yr	5yr	10yr	25yr	50yr	100yr
Flooded area	m^2	1008000	1515000	2000000	2808000	3502000	4530000
	ha	100.8	151.5	200	280	350.2	453

Table 4.3 shows the flood inundation area is increasing from year to year. The flooded area increases from 100.8 to 151.5 ha if we take into account the 2 and 5 year return periods. This suggests that during the course of three years, the flooded area grew by 50.7%. The farmers lost 50.7 ha of agricultural land throughout these three years. It is approximately 453 ha when the area is inundated at the 100-year return period. When this amount is divided by the length of the river (4600 m), the width become 965 m. This indicates that the flood will extend up to a distance 482.5 meters to both riverside.

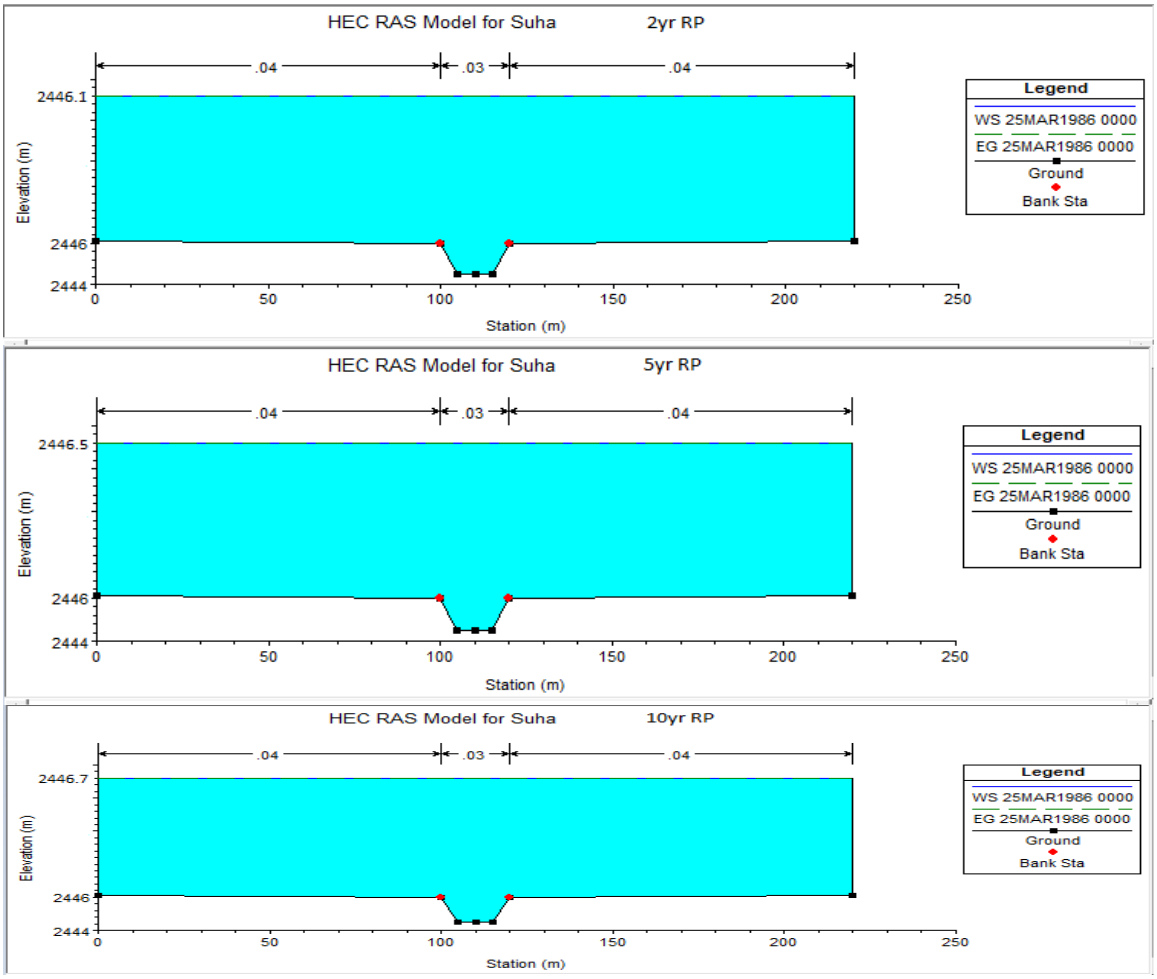

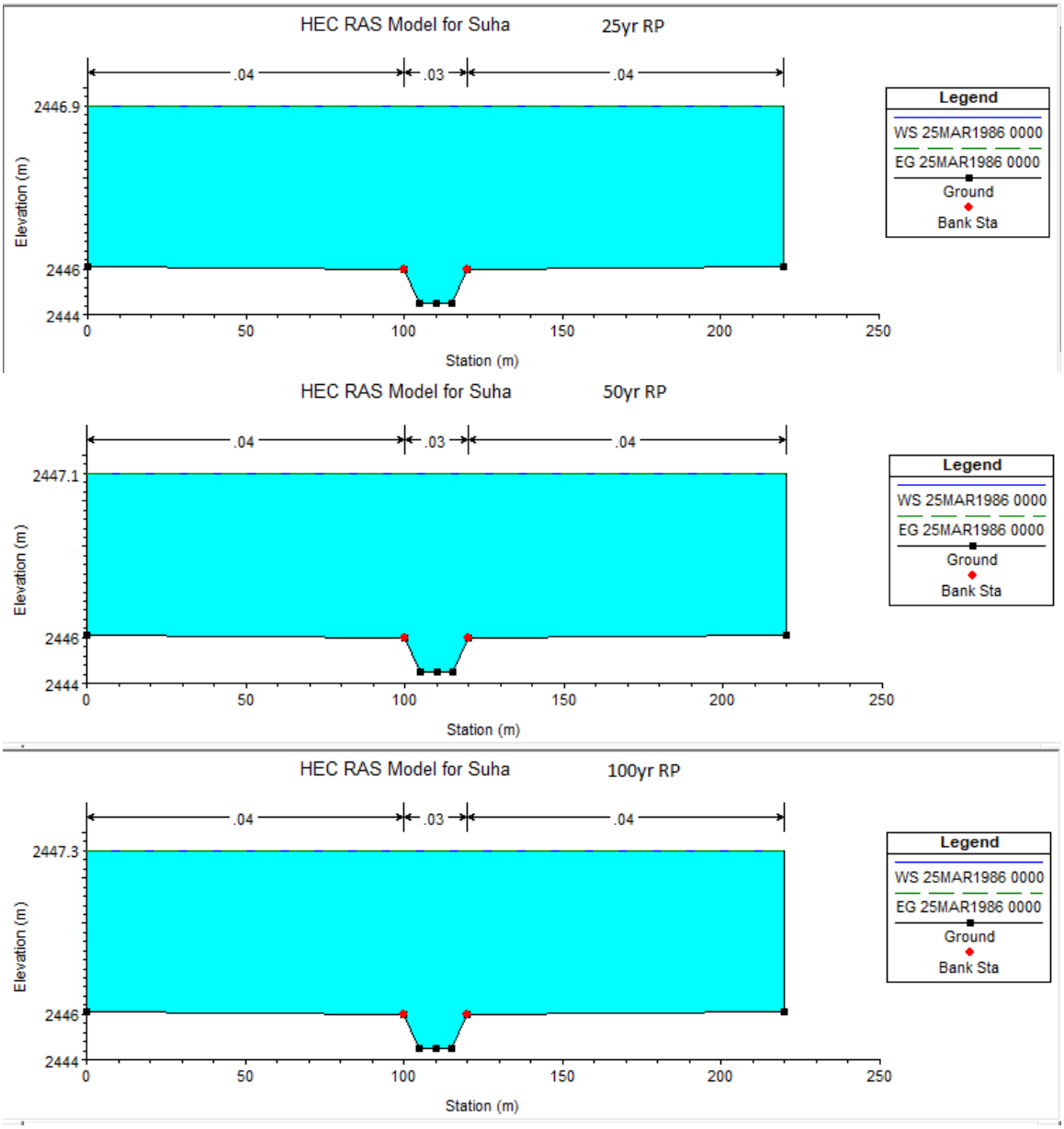

Figure 4.8: Cross sectional water surface elevation at different return period

Figure 4.8 shows the cross sectional water surface elevation at different return periods. For instance at 2yr return period the water surface above the ground surface outside the river is 10cm and at 5yr return period it is going to be 50 cm depth.

4.5 Flood vulnerable areas from the selected river section

The flood extent is not uniform throughout the whole river. Some areas are highly affected, whereas others are flooded to some extent. As the RAS mapper shows us, from the selected 4.6 km of river length, some stations are highly flooded. These Stations are station 5, 39, 40, 52, 53 and station 64. These stations are more flood vulnerable stations from the other stations at 2 year, 5 year, 10 year, and 25 year return periods. However at 50 and 100 year return periods almost all station will be vulnerable and highly flooded stations.

As Figure 4.9 shows, some stations are highly flooded while others not. This variability in inundation area is due to the variation in the depth of the river at each station. When the river depth is shallow, the flood carrying capacity of the river will be lower, and vice versa. If the river's capacity is insufficient to carry the incoming flood, the flood will overflow and flow to the sides of the river. The stations listed in Figure 4.9 have relatively shallow depths, so the flood-inundated area is higher.

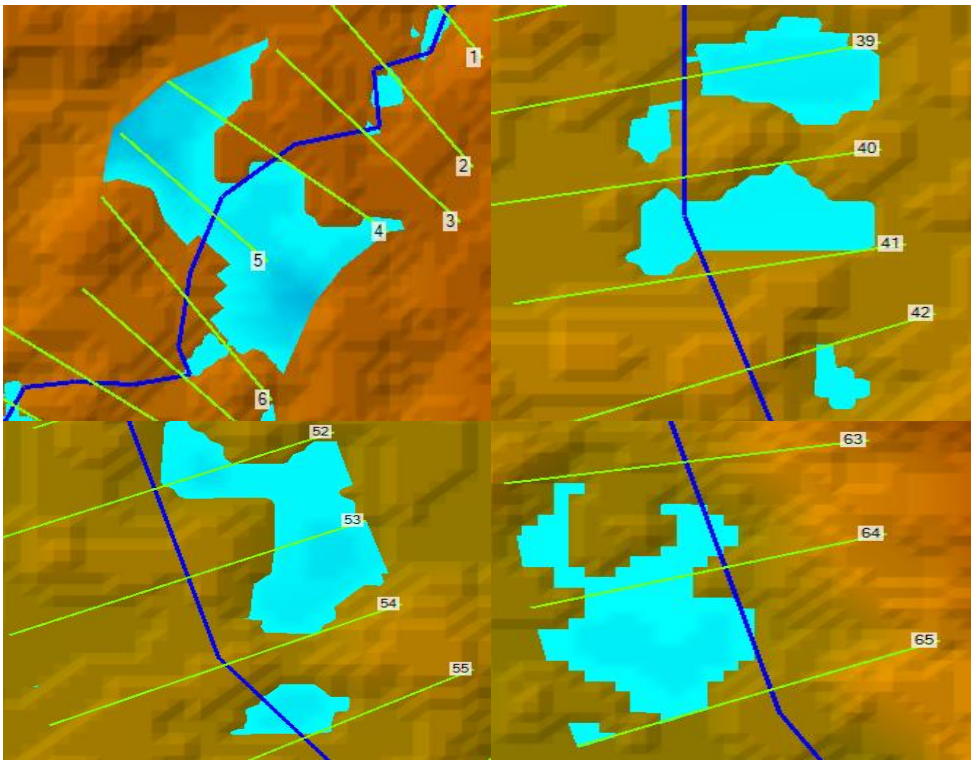

Figure 4.9: Flood vulnerable stations

5. CONCLUSION AND RECOMMENDATIONS

5.1 Conclusion

This thesis work was conducted to assess the flooding problem on river sides or flood plain areas and its risk. Both hydrological (HEC HMS) and hydraulic (HEC RAS) models were calibrated and validated to compute peak flood at different return periods, which was also the aim of this thesis work. The final target of this thesis work was to prepare a flood inundation map of the Suha flood plain by using the hydraulic model HEC RAS.

Different data collection methods and two data types were used for this study. Primary data like river cross-section and interviews and secondary data such as meteorological data, hydrological data, DEM data, land use and land cover data, and soil type data were collected and a total of nineteen years of daily stream flow and rainfall data were used. From nineteen years of observed stream flow data, the first thirteen years has been used for calibration and the remaining six years for validation.

After the calibration and validation of the HEC HMS model, the performance indicators showed that the model was found to be very good. The performance of the hydrological model (HEC HMS) and hydraulic model (HEC RAS) was checked with their own performance evaluation methods. The HEC HMS model calibration was evaluated by the Nash Sutcliffe Efficiency, percent of bias, and root mean square error and values of 0.723, 10.83, and 0.57, respectively, were observed. The peak flood magnitude obtained for 2, 5, 10, 25, 50, and 100 years return periods were 50.4, 76.1, 107, 151.9, 211, and 301 m^3/s, respectively.

On the other hand, the HEC RAS model calibration and validation results were compared with the satellite image, and a relatively good result was obtained. The calibrated Manning roughness for the left and right banks obtained was 0.04, and for the main channel of the river, it was 0.03. The HEC RAS model result shows that the flood inundation map covers 100.8, 151.5, 200, 280, 350.2, and 453 ha for 2, 5, 10, 25, 50, and 100 year return periods, respectively. This result indicates that the inundated area is expected to increase with time. Especially for the last two return periods, the flood

magnitude is too high, and the corresponding inundated area is going to be wide. This implies that an appropriate mitigation measure has to be taken to overcome the problem.

5.2 Recommendations

Depending on the results obtained from the HEC RAS model for different return periods, the flood-inundated area increases, especially for 50 to 100 year return periods. Therefore, the following mitigation measures were recommended for dwellers and the concerned government bodies.

- In order to minimize the flood risk, magnitude of the flood, and damages to crops, it is better to adopt both structural measures like constructing a dike and non-structural measures such as soil conservation practices, appropriate land use, and land cover practices.
- Give awareness to the local people to protect their agricultural land through practicing land conservation, especially by focusing on more vulnerable areas.
- Research on flood prediction and mitigation measures in the specific study area should be motivated and appreciated to reduce the flood risk.
- It is recommended to perform flood damage analysis study using (HEC-FDA model) to determine a suitable structure type for the flood prone areas.

REFERENCES

Agarwal, C. (2002). A review and assessment of land-use change models: dynamics of space, time, and human choice.

Amede, T., Belachew, T., & Geta, E. (2001). Reversing the degradation of arable land in the Ethiopian highlands. managing Africa's soils; no. 23.

Ahern, M., & Kovats, R. S. (2006). The Health Impacts of Floods: Responding to Present and Future Risks. Flood Hazards and Health. Earthscan, London.

Ahern, M., Kovats, R. S., Wilkinson, P., Few, R., & Matthies, F. (2005). Global health impacts of floods: epidemiologic evidence. Epidemiologic Reviews, 27(1), 36–46.

Alemu, M. M., Bawoke, G. T. J. J. O. W. & Change, C. 2020. Analysis of spatial variability and temporal trends of rainfall in Amhara region, Ethiopia. 11, 1505-1520.

Arsenault, K. R., Kumar, S. V., Geiger, J. V., Wang, S., Kemp, E., Mocko, D. M., Beaudoing, H. K., Getirana, A., Navari, M. & Li, B. J. G. M. D. 2018. The land surface data toolkit (ldt v7. 2)–a data fusion environment for land data assimilation systems. 11, 3605-3621.

Assefa, A. & Abunna, F. J. V. M. I. 2018. Maintenance of fish health in aquaculture: review of epidemiological approaches for prevention and control of infectious disease of Fish. 2018.

Awal, R. J. M. T., Trishuvan University, Nepal 2003. Application of steady and unsteady flow model and gis for floodplain analysis and risk mapping: a case study of Lakhandei River, Nepal.

Bishaw, K. (2012). Application of GIS and remote sensing techniques for flood Hazard and risk assessment: The case of Dugeda bora Woreda of Oromiya regional state, Ethiopia.

Billi, P., Tadesse, Y., & Rossano, A. (2015). Increased frequency of flash floods in Dire Dawa , Ethiopia : Change in rainfall intensity or human impact ? 1373–1394. https://doi.org/10.1007/s11069-014-1554-0

Biondi, D., Freni, G., Iacobellis, V., Mascaro, G., & Montanari, A. (2012). Validation of Hydrological models: conceptual basis, methodological approaches and a proposal for a code of practice. physics and chemistry of the earth, parts A/B/C, 42, 70–76.

Bornhöft, A., Hanke-Rauschenbach, R., & Sundmacher, K. (2013). Steady-state analysis of the anaerobic digestion model no. 1 (Adm1). Nonlinear Dynamics, 73, 535–549.

Brandon, T. O. J. E. L. 2016. Nationwide permit 13, shoreline armoring, and the important role of the us army corps of engineers in coastal climate change adaptation. 46, 537.

Bule Hora, E. & Hora, E. 2020. Flooding in Ethiopia; Causes, impact and coping mechanisms. a review.

Burrell, B., Huokuna, M., Beltaos, S., Kovachis, N., Turcotte, B. & Jasek, M. Flood Hazard And Risk delineation of ice-related floods: present status and outlook. proceedings of the 18th cguhs cripe workshop on the hydraulics of ice covered Rivers, Quebec City, Qc, Canada, 2015. 18-20.

Charrier, R. & Li, Y. J. A. G. 2012. Assessing Resolution And Source Effects of Digital Elevation Models on Automated Floodplain Delineation: A Case Study From The Camp Creek Watershed, Missouri. 34, 38-46.

Council, N. R. 2007. Elevation data for floodplain mapping, national academies press.

Collischonn, B., Collischonn, W., & Tucci, C. E. M. (2008). Daily hydrological modeling in the amazon basin using trmm rainfall estimates. journal of hydrology, 360(1–4), 207–216.

Cunnane, C. (1988). Methods and merits of regional flood frequency analysis. journal of hydrology, 100(1–3), 269–290.

Demessie, D. A. 2007. Assessment of flood risk in Dire Dawa town, eastern Ethiopia, Using Gis. Addis Ababa University.

Dubale, P. (2001). Soil and Water resources and degradation factors affecting productivity in Ethiopian highland agro-ecosystems. northeast African studies, 27–51.

Erena, S. H., & Worku, H. (2018). Flood risk analysis: causes and landscape based mitigation strategies in Dire Dawa city, Ethiopia. Geoenvironmental Disasters, 5(1), 1–19.

Fleming, M. & Brauer, T. J. U. A. C. O. E., Institute of water resources. Https://Www. Hec. Usace. Army. Mil/Software/HEC-HMS/Documentation/HEC-HMS_Quickstart_Guide_4 2016a. Hydrologic modelling system hec-hms quick start guide.[Online] Version 4.2.

Fleming, M. & Brauer, T. J. U. A. C. O. E. I. O. W. R. H. E. C., Cpd-74d 2016b. Hydrologic modeling system HEC-HMS Quick Start Guide.

Gaál, L., Szolgay, J., Kohnová, S., Parajka, J., Merz, R., Viglione, A. & Blöschl, G. J. W. R. R. 2012. Flood timescales: understanding the interplay of climate and catchment processes through comparative hydrology. 48.

Gebre, S. L. J. H. C. R. 2015. Application of the hec-hms model for runoff simulation of upper Blue Nile River Basin. 6, 1.

Getahun, Y., Gebre, S. J. J. O. C. & Engineering, E. 2015. Flood hazard assessment and mapping of flood inundation area of the Awash River Basin in Ethiopia Using Gis and Hec-Georas/Hec-Ras Model. 5, 1.

Geremew, G. M., Mini, S., & Abegaz, A. (2020). Spatiotemporal variability and trends in rainfall extremes in Enebsie Sar Midir District, Northwest Ethiopia. Modeling earth systems and environment, 6, 1177–1187.

Greenough, G., McGeehin, M., Bernard, S. M., Trtanj, J., Riad, J., & Engelberg, D. (2001). The potential impacts of climate variability and change on health impacts of extreme weather events in the United States. Environmental Health Perspectives, 109(suppl 2), 191–198.

Gilard, O. 1996. Flood risk management: risk cartography for objective negotiations,[In:] Third Ihp/Iahs George Kovacs Colloquium. Unesco, Paris,(19–21 Sept. 1996).

Goodell, C. R. & Brunner, G. W. 2004. Watershed analysis with the Hydrologic Engineering Center's River Analysis System (Hec-Ras). Engineer research and development center vicksburg Ms.

Hosking, J. & Wallis, J. J. N. Y., Ny 1997. Regional frequency analysis: an approach based on L-Moments.© Cambridge University Press.

Hua, A. K. J. I. J. S. E. R. 2014. Monsoon flood disaster in kota bharu, kelantan case study: a comprehensive review. 3, 2347-3878.

Hua, F., West, J. R., Barker, R. A., & Forster, C. F. (1999). Modelling of chlorine decay in municipal water supplies. water research, 33(12), 2735–2746.

Hunter, P. R. (2003). Climate change and waterborne and vector-borne disease. Journal of Applied Microbiology, 94(s1), 37–46.

Hussain, A., Trudell, P., & Repta, A. J. (1970). Quantitative spectrophotometric methods for determination of sodium hypochlorite in aqueous solutions. journal of pharmaceutical sciences, 59(8), 1168–1170.

Halwatura, D., & Najim, M. M. M. (2013). Application of the hec-hms model for runoff simulation in a tropical catchment. environmental modelling & software, 46, 155–162.

Hanson, J. D., Rojas, K. W., & Shaffer, M. J. (1999). Calibrating The root zone water quality model. agronomy journal, 91(2), 171–177.

Hunziker, S., Gubler, S., Calle, J., Moreno, I., Andrade, M., Velarde, F., Ticona, L., Carrasco, G., Castellón, Y., & Oria, C. (2017). Identifying, attributing, and overcoming common data quality issues of manned station observations. international journal of climatology, 37(11), 4131–4145.

Jacinto, R., Grosso, N., Reis, E., Dias, L., Santos, F. D., & Garrett, P. (2015). Continental Portuguese territory flood susceptibility index–contribution to a vulnerability index. Natural Hazards and Earth System Science, 15(8), 1907–1919.

Kumar, A., Kanga, S., Taloor, A. K., Singh, S. K., & Đurin, B. (2021). Surface runoff estimation of sind river basin using integrated scs-cn and gis techniques. hydroresearch, 4, 61–74.

Legese, B. (2022). Flooding in Ethiopia ; Causes , Impact , and Coping Mechanism . A Review. September 2020.

Legese, B., Gumi, B., & Bule Hora, E. (2020). Flooding in Ethiopia; causes, impact and coping mechanisms. A review. International Journal of Research and Analytical Reviews, 7(3), 707–717.

Lehner, B., & Grill, G. (2013). Global river hydrography and network routing: baseline data and new approaches to study the world's large river systems. hydrological processes, 27(15), 2171–2186.

Manandhar, B. J. M. O. S. T. I. W. M. T. U. I. O. F. P., Nepal 2010. Flood plain analysis and risk assessment of Lothar Khola.

Mandych, A. J. I. O. G., Moscow, Russia 2005. Natural disasters–vol. classification of floods-department of physical geography and land-use.

Monroe, J., Ramsey, E., & Berglund, E. (2018). Allocating countermeasures to defend water distribution systems against terrorist attack. reliability engineering & system safety, 179, 37–51.

Moriasi, D. N., Gitau, M. W., Pai, N., & Daggupati, P. (2015). Hydrologic and water quality models: performance measures and evaluation criteria. transactions of the Asabe, 58(6), 1763–1785.

Odyuo, N. M. (2020). Modelling the impact of land use land cover changes on th runoff processes of chalakudy basin using Hec-Hms Model. Department of Ide.

Okonofua, E. S., Atikpo, E., Lasisi, K. H., Oladosu, O. S., Uwadia, N. J. M. E. S. & Environment 2022. Application of selected ffa methods in extreme flood prediction of River Osse. 1-15.

Orale, R. L. J. C. D. R. J. 2015. Flood risk assessment in post antiao river control project in catbalogan city, Philippines. 3, 39-52.

Osti, R. & Egashira, S. J. H. P. A. I. J. 2008. Method to improve the mitigative effectiveness of a series of check dams against debris flows. 22, 4986-4996.

Ouma, Y. O. & Tateishi, R. J. W. 2014. Urban flood vulnerability and risk mapping using integrated multi-parametric AHP and GIS: methodological overview and case study assessment. 6, 1515-1545.

Patel, A. D., Patel, D. P. & Prakash, I. Flood modelling using HEC-RAS and geo-informatics technology in lower reaches of Shetrunji river, gujarat, India. proceedings of national conference on water resources & flood management with special reference to flood modeling, 2016.

Pappenberger, F., Matgen, P., Beven, K. J., Henry, J.-B., & Pfister, L. (2006). Influence of uncertain boundary conditions and model structure on flood inundation predictions. advances in water resources, 29(10), 1430–1449.

Porter, J. W., & Mcmahon, T. A. (1971). A model for the simulation of streamflow data from climatic records. journal of Hydrology, 13, 297–324.

Pilgrim, D. J. W. R. R. 1976. Travel times and nonlinearity of flood runoff from tracer measurements on a small watershed. 12, 487-496.

Raford, N. & Ragland, D. J. T. R. R. 2004. Space syntax: innovative pedestrian volume modeling tool for pedestrian safety. 1878, 66-74.

Rimas, A., & Fraser, E. (2010). Empires of food: feast, famine, and the rise and fall of civilizations. simon and schuster.

Raspati, G. S., Azrague, K., & Jotte, L. (2017). Review of stormwater management practices.

Retsinis, E., Daskalaki, E., & Papanicolaou, P. (2020). Dynamic flood wave routing in prismatic channels with hydraulic and hydrologic methods. journal of water supply: research and technology-aqua, 69(3), 276–287.

Rosegrant, M. W., Ringler, C., Mckinney, D. C., Cai, X., Keller, A., & Donoso, G. (2000). Integrated economic-hydrologic water modeling at the basin scale: the Maipo river basin. agricultural economics, 24(1), 33–46.

Semaw, F., Zeleke, G. & Balew, A. J. A. G. 2022. Evaluating flood risk management practices and vulnerability mapping in alawuha watershed (North Wollo Zone, Ethiopia) using GIS and remote sensing. 1-21.

Shende, S. 2006. Database-driven hydraulic simulation of canal irrigation networks using object-oriented high-resolution methods. loughborough university.

Shrestha, B. R., Rai, R. K. & Marasini, S. J. T. G. B. 2020. Review of flood hazards studies in Nepal. 7, 24-32.

Sinha, S., Chandel, S. J. R. & Reviews, S. E. 2014. Review of software tools for hybrid renewable energy systems. 32, 192-205.

Smit, B. & Pilifosova, O. J. S. D. 2003. Adaptation to climate change in the context of sustainable development and equity. 8, 9.

Srinivasan, R. & Arnold, J. G. J. J. J. O. T. A. W. R. A. 1994. Integration of a basin-scale water quality model with GIS 1. 30, 453-462.

Scherrer, S., & Naef, F. (2003). A decision scheme to indicate dominant hydrological flow processes on temperate grassland. hydrological processes, 17(2), 391–401.

Subramanya, K. (2008). Engineering Hydrology. Mcgraw-Hill.

Sumarauw, J. S. F., & Ohgushi, K. (2012). Analysis on curve number, land use and land cover changes and the impact to the peak flow in the Jobaru river basin, Japan. international journal of civil & environmental engineering ijcee-ijens, 12(02), 17–23.

Tabari, H., Somee, B. S., & Zadeh, M. R. (2011). Testing for long-term trends in climatic variables in iran. atmospheric research, 100(1), 132–140.

Thu, K. C. M., Zin, W. W., & Khine, E. E. (2019). Simulation of rainfall-runoff process using HEC-HMS model for chindwin river basin. proceedings of national conference of science and Engineering, 27–28.

Undro's, M. N. D. J. A. M. F. P. M. & Nations, P. U. 1991. Phenomena, effects and options.28.

Van Chinh, L., Iseri, H., Hiramatsu, K., Harada, M., & Mori, M. (2013). Simulation of rainfall runoff and pollutant load for Chikugo river basin in japan using a GIS-based distributed parameter model. paddy and water environment, 11, 97–112.

Wakjira, M. T., Peleg, N., Anghileri, D., Molnar, D., Alamirew, T., Six, J., & Molnar, P. (2021). Rainfall seasonality and timing: implications for cereal crop production in Ethiopia. agricultural and forest meteorology, 310, 108633.

Wisner, B. (2004). At risk: natural hazards, people's vulnerability and disasters. Psychology Press

Ys, G. & Gebre, S. 2015. Journal of Civil & Environmental Engineering.

Yuan, Y. & Qaiser, K. 2011a. Floodplain Modeling in The Kansas River Basin Using Hydrologic Engineering Center (HEC) Models: impacts of urbanization and wetlands for mitigation, us environmental protection agency, office of research and development.

Yuan, Y. & Qaiser, K. J. U. E. P. A. L. V., Nv, Usa 2011b. Floodplain modeling in the Kansas river basin using Hydrologic Engineering Center (HEC) Models.

APPENDICES

APPENDIX A: Sample photos during field data collection

APPENDIX B1

Subbasins	Major Soil Type	MajorLC	HSG	Area(km^2)
1	Vertisols	Built Up Area	D	52.57
	Luvisols	Cultivated Land	B	
	Lithosols	Forest Land	D	
	Rendzians	Grass Land	D	
	Cambisols	Shrub and Bush Land	B	
2	Luvisols	Cultivated Land	B	154
	Lithosols	Forest Land	D	
	Rendzians	Grass Land	D	
3	Vertisols	Built Up Area	D	27.806
	Luvisols	Cultivated Land	B	
	Lithosols	Forest Land	D	
	Rendzians	Grass Land	D	
4	Vertisols	Built Up Area	D	31.541
	Luvisols	Cultivated Land	B	
	Lithosols	Forest Land	D	
	Rendzians	Grass Land	D	
5	Luvisols	Cultivated Land	B	27.738
	Lithosols	Forest Land	D	
	Rendzians	Grass Land	D	
6	Luvisols	Cultivated Land	B	32.613
	Lithosols	Forest Land	D	
	Rendzians	Grass Land	D	

7	Vertisols	Built Up Area	D	67.384
	Luvisols	Cultivated Land	B	
	Lithosols	Forest Land	D	
	Rendzians	Grass Land	D	
8	Vertisols	Built Up Area	D	21.444
	Luvisols	Cultivated Land	B	
	Lithosols	Forest Land	D	
	Rendzians	Grass Land	D	
9	Vertisols	Built Up Area	D	65.061
	Luvisols	Cultivated Land	B	
	Lithosols	Forest Land	D	
	Rendzians	Grass Land	D	
10	Vertisols	Built Up Area	D	21.639
	Luvisols	Cultivated Land	B	
	Lithosols	Forest Land	D	
	Rendzians	Grass Land	D	
11	Vertisols	Built Up Area	D	287.99
	Luvisols	Cultivated Land	B	
	Lithosols	Forest Land	D	
	Rendzians	Grass Land	D	
	Cambisols	Shrub and Bush Land	B	

APPENDIX B2

Subbasins	Major Soil Type	MajorLC	HSG	CNi	Ai	CN*Ai	Sum (CNi*Ai)	Sum (Ai)	Comp CN
1	Vertisols	Built Up Area	D	85	26.285	2234.225	4235.0392	52.57	80.56
	Luvisols	Cultivated Land	B	75	5.257	394.275			
	Lithosols	Forest Land	D	77	10.514	809.578			
	Rendzians	Grass Land	D	80	4.2056	336.448			
	Cambisols	Shrub and Bush Land	B	73	6.3084	460.5132			
2	Luvisols	Cultivated Land	B	75	77	5775	11842.6	154	76.9
	Lithosol	Forest	D	77	30.8	2371.6			

	s	Land							
	Rendzians	Grass Land	D	80	46.2	3696			
3	Vertisols	Built Up Area	D	85	2.22448	189.0808	2156.07724	27.806	77.54
	Luvisols	Cultivated Land	B	75	13.903	1042.725			
	Lithosols	Forest Land	D	77	3.33672	256.9274			
	Rendzians	Grass Land	D	80	8.3418	667.344			
4	Vertisols	Built Up Area	D	85	2.52328	214.4788	2445.68914	31.541	77.54
	Luvisols	Cultivated Land	B	75	15.7705	1182.788			
	Lithosols	Forest Land	D	77	3.78492	291.4388			
	Rendzians	Grass Land	D	80	9.4623	756.984			
5	Luvisols	Cultivated Land	B	75	13.869	1040.175	2133.0522	27.738	76.9
	Lithosols	Forest Land	D	77	5.5476	427.1652			
	Rendzians	Grass Land	D	80	8.3214	665.712			
6	Luvisols	Cultivated Land	B	75	16.3065	1222.988	2507.9397	32.613	76.9
	Lithosols	Forest Land	D	77	6.5226	502.2402			
	Rendzians	Grass Land	D	80	9.7839	782.712			
7	Vertisols	Built Up Area	D	85	5.39072	458.2112	5224.95536	67.384	77.54
	Luvisols	Cultivated Land	B	75	33.692	2526.9			
	Lithosols	Forest Land	D	77	8.08608	622.6282			
	Rendzians	Grass Land	D	80	20.2152	1617.216			
8	Vertisols	Built Up Area	D	85	1.71552	145.8192	1662.76776	21.444	77.54
	Luvisols	Cultivat	B	75	10.722	804.15			

		ed Land							
	Lithosols	Forest Land	D	77	2.57328	198.1426			
	Rendzians	Grass Land	D	80	6.4332	514.656			
9	Vertisols	Built Up Area	D	85	5.20488	442.4148	5044.82994	65.061	77.54
	Luvisols	Cultivated Land	B	75	32.5305	2439.788			
	Lithosols	Forest Land	D	77	7.80732	601.1636			
	Rendzians	Grass Land	D	80	19.5183	1561.464			
10	Vertisols	Built Up Area	D	85	1.73112	147.1452	1677.88806	21.639	77.54
	Luvisols	Cultivated Land	B	75	10.8195	811.4625			
	Lithosols	Forest Land	D	77	2.59668	199.9444			
	Rendzians	Grass Land	D	80	6.4917	519.336			
11	Vertisols	Built Up Area	D	85	143.995	12239.58	23200.4744	287.99	80.56
	Luvisols	Cultivated Land	B	75	28.799	2159.925			
	Lithosols	Forest Land	D	77	57.598	4435.046			
	Rendzians	Grass Land	D	80	23.0392	1843.136			
	Cambisols	Shrub and Bush Land	B	73	34.5588	2522.792			

APPENDIX B3

Subbasins	Major Soil Type	MajorLC	HSG	CNi	Comp CN	S	Ia
1	Vertisols	Built Up Area	D	85	80.56	569.2929	113.8586
	Luvisols	Cultivated Land	B	75			
	Lithosols	Forest Land	D	77			
	Rendzians	Grass Land	D	80			
	Cambisols	Shrub and Bush Land	B	73			
2	Luvisols	Cultivated Land	B	75	76.9	584.2991	116.8598
	Lithosols	Forest Land	D	77			
	Rendzians	Grass Land	D	80			
3	Vertisols	Built Up Area	D	85	77.54	581.5729	116.3146
	Luvisols	Cultivated Land	B	75			
	Lithosols	Forest Land	D	77			
	Rendzians	Grass Land	D	80			
4	Vertisols	Built Up Area	D	85	77.54	581.5729	116.3146
	Luvisols	Cultivated Land	B	75			
	Lithosols	Forest Land	D	77			
	Rendzians	Grass Land	D	80			
5	Luvisols	Cultivated Land	B	75	76.9	584.2991	116.8598
	Lithosols	Forest Land	D	77			
	Rendzians	Grass Land	D	80			
6	Luvisols	Cultivated Land	B	75	76.9	584.2991	116.8598
	Lithosols	Forest Land	D	77			
	Rendzians	Grass Land	D	80			
7	Vertisols	Built Up Area	D	85	77.54	581.5729	116.3146
	Luvisols	Cultivated Land	B	75			
	Lithosols	Forest Land	D	77			
	Rendzians	Grass Land	D	80			
8	Vertisols	Built Up Area	D	85	77.54	581.5729	116.3146
	Luvisols	Cultivated Land	B	75			
	Lithosols	Forest Land	D	77			
	Rendzians	Grass Land	D	80			
9	Vertisols	Built Up Area	D	85	77.54	581.5729	116.3146
	Luvisols	Cultivated Land	B	75			
	Lithosols	Forest Land	D	77			
	Rendzians	Grass Land	D	80			
10	Vertisols	Built Up Area	D	85	77.54	581.572	116.314

	Luvisols	Cultivated Land	B	75		9	6
	Lithosols	Forest Land	D	77			
	Rendzians	Grass Land	D	80			
11	Vertisols	Built Up Area	D	85	80.56	569.2929	113.8586
	Luvisols	Cultivated Land	B	75			
	Lithosols	Forest Land	D	77			
	Rendzians	Grass Land	D	80			
	Cambisols	Shrub and Bush Land	B	73			

APPENDIX B4

Sub-basins	Parameters	unit	Value
1	Area (A)	km^2	52.57
	Curve number (CN)		80.58
	Initial abstraction (Ia)	mm	113.86
	Imperviousness	%	5
2	Area (A)	km^2	154
	Curve number (CN)		76.9
	Initial abstraction (Ia)	mm	116.86
	Imperviousness	%	5
3	Area (A)	km^2	27.81
	Curve number (CN)		77.54
	Initial abstraction (Ia)	mm	116.31
	Imperviousness	%	5
4	Area (A)	km^2	31.54
	Curve number (CN)		77.54
	Initial abstraction (Ia)	mm	116.31
	Imperviousness	%	5
5	Area (A)	km^2	27.74
	Curve number (CN)		76.9
	Initial abstraction (Ia)	mm	116.86
	Imperviousness	%	5
6	Area (A)	km^2	32.61
	Curve number (CN)		76.9

	Initial abstraction (Ia)	mm	116.86
	Imperviousness	%	5
7	Area (A)	km^2	67.38
	Curve number (CN)		77.54
	Initial abstraction (Ia)	mm	116.31
	Imperviousness	%	5
8	Area (A)	km^2	21.44
	Curve number (CN)		77.54
	Initial abstraction (Ia)	mm	116.31
	Imperviousness	%	5
9	Area (A)	km^2	65.06
	Curve number (CN)		77.54
	Initial abstraction (Ia)	mm	116.31
	Imperviousness	%	5
10	Area (A)	km^2	21.64
	Curve number (CN)		77.54
	Initial abstraction (Ia)	mm	116.31
	Imperviousness	%	5
11	Area (A)	km^2	287.99
	Curve number (CN)		80.56
	Initial abstraction (Ia)	mm	113.86
	Imperviousness	%	5

APPENDIX : C Monthly rainfall of some stations

APPENDIX : C1 Monthly rainfall of Bichena Station

year	Jan	Feb	Mar	Apr	May	Jun	Jul	Aug	Sep	Oct	Nov	Dec
1986	8.8	0.0	0.0	26.8	31.9	50.1	252.0	179.4	28.0	136.5	0.0	3.2
1987	0.0	21.4	126.8	34.5	115.4	89.3	249.0	343.2	95.9	62.1	0.0	2.0
1988	15.9	66.5	0.0	33.3	10.5	105.3	655.8	182.8	219.3	49.2	0.0	0.0
1989	0.0	3.6	22.7	63.6	15.4	68.1	124.2	366.3	125.6	19.5	6.6	0.0
1990	30.2	7.6	48.4	27.4	20.6	0.0	385.8	114.1	58.2	32.4	6.6	0.0
1991	3.8	7.6	22.7	33.3	31.9	47.6	175.3	131.1	58.2	32.4	6.6	4.8
1992	9.0	47.1	18.8	96.0	47.7	53.7	228.6	313.8	176.2	131.4	0.0	23.5
1993	2.5	23.0	31.7	83.9	158.8	85.5	367.5	79.2	140.9	33.3	0.0	0.0
1994	1.4	2.4	27.3	40.6	25.2	100.3	416.5	253.6	104.7	0.0	4.2	0.0

1995	0.0	9.7	15.4	81.5	79.2	20.2	262.5	244.3	34.9	0.8	0.0	34.4
1996	15.2	0.4	94.4	100.4	95.5	157.5	215.2	202.3	46.2	3.6	21.5	1.4
1997	36.8	0.0	26.9	154.4	49.0	90.5	228.0	180.2	43.9	136.3	45.6	7.2
1998	1.2	12.0	33.4	15.8	134.5	80.2	271.5	261.0	122.8	141.5	2.1	0.0
1999	13.1	0.0	1.5	34.7	31.9	47.9	314.1	313.9	40.5	144.3	1.5	2.2
2000	0.0	0.0	0.9	111.5	31.9	65.2	302.8	250.1	151.9	55.2	81.1	11.2
2001	0.0	11.3	96.6	46.3	86.5	147.0	419.0	224.8	44.1	5.9	1.7	3.0
2002	23.8	21.2	17.9	23.5	6.4	71.4	270.5	168.5	67.4	32.4	0.0	38.4
2003	7.8	18.1	74.9	33.1	0.0	168.7	242.4	249.9	122.3	16.7	27.5	29.5
2004	10.5	6.8	42.0	52.7	41.6	113.6	175.6	189.4	65.5	32.2	0.2	4.8

APPENDIX : C2 Monthly rainfall of Debrewerk Station

year	Jan	Feb	Mar	Apr	May	Jun	Jul	Aug	Sep	Oct	Nov	Dec
1986	0.0	24.6	61.2	55.6	19.4	139.5	178.0	206.5	142.4	99.1	11.2	15.4
1987	2.1	9.3	89.5	43.1	115.5	79.7	134.9	253.4	52.6	45.9	15.6	11.5
1988	15.9	66.5	0.0	46.8	10.5	105.3	655.8	182.8	219.3	49.2	0.2	0.0
1989	11.3	9.8	76.5	81.8	29.5	62.8	175.2	196.8	93.3	3.0	4.9	101.0
1990	1.7	36.5	51.0	48.6	48.2	27.7	171.3	123.0	81.0	2.0	1.6	0.0
1991	19.8	6.5	20.7	0.6	47.2	188.2	340.9	160.3	74.1	3.8	5.3	3.6
1992	10.0	20.8	34.0	47.4	54.2	25.5	140.1	182.8	33.2	77.1	40.1	35.4
1993	1.3	19.3	50.6	74.2	136.7	50.7	190.9	113.4	89.6	47.1	6.5	0.0
1994	0.0	24.9	14.1	23.3	47.3	48.2	283.2	244.1	80.2	2.0	0.6	0.0
1995	0.3	10.2	28.7	33.0	105.2	37.3	234.2	305.0	66.3	6.0	4.4	34.6
1996	42.0	0.0	63.6	137.4	84.3	154.9	191.9	184.2	74.8	0.0	15.1	0.0
1997	9.1	0.0	54.7	46.8	56.5	79.7	230.1	105.7	147.3	151.3	12.0	14.5
1998	9.1	16.3	35.5	10.3	144.2	126.5	305.4	362.4	92.0	147.2	12.0	0.0
1999	8.8	0.0	0.0	26.8	56.5	50.1	252.0	179.4	28.0	136.5	0.0	3.2
2000	0.0	0.0	9.0	114.3	36.4	71.0	373.6	397.9	126.8	107.1	62.5	36.0
2001	0.0	24.0	84.8	25.1	81.2	107.3	310.0	362.7	76.3	19.5	0.0	5.0
2002	15.2	6.8	78.7	4.3	0.0	41.9	252.8	200.2	34.5	0.0	0.0	5.4
2003	15.0	68.0	101.9	7.2	3.0	98.2	252.3	227.8	94.9	34.2	19.4	12.9
2004	7.8	6.3	23.4	63.0	7.6	46.0	252.3	286.8	71.6	92.7	6.6	12.4

APPENDIX : C3 Monthly rainfall of F/Berhan Station

year	Jan	Feb	Mar	Apr	May	Jun	Jul	Aug	Sep	Oct	Nov	Dec
1986	8.5	75.1	26.1	77.6	29.9	169.1	167.1	208.4	172.8	35.5	0.0	0.0
1987	0.0	21.4	126.8	34.5	180.0	89.3	249.0	106.6	95.9	62.1	0.0	2.0
1988	18.3	41.9	0.0	26.3	11.4	93.4	382.4	106.6	216.2	113.5	0.0	0.3
1989	0.0	18.7	159.9	117.9	43.1	103.2	106.6	106.6	215.2	69.5	0.0	65.1
1990	1.7	36.5	51.0	48.6	48.2	27.7	171.3	123.0	81.0	2.0	1.6	0.0
1991	19.8	6.5	20.7	0.6	47.2	188.2	340.9	106.6	106.6	3.8	5.3	3.6
1992	10.0	20.8	34.0	47.4	54.2	25.5	140.1	182.8	33.2	77.1	40.1	35.4
1993	1.3	19.3	106.6	74.2	136.7	50.7	190.9	113.4	89.6	47.1	6.5	0.0
1994	0.0	24.9	14.1	23.3	47.3	48.2	283.2	244.1	80.2	106.6	0.6	0.0
1995	0.3	10.2	28.7	106.6	105.2	37.3	234.2	305.0	66.3	6.0	4.4	34.6
1996	42.0	0.0	63.6	137.4	84.3	154.9	191.9	184.2	74.8	0.0	15.1	0.0
1997	9.1	0.0	106.6	46.8	56.5	79.7	230.1	105.7	147.3	151.3	12.0	14.5
1998	9.1	16.3	35.5	10.3	144.2	106.6	305.4	362.4	92.0	147.2	12.0	0.0
1999	8.8	0.0	0.0	26.8	56.5	50.1	252.0	179.4	28.0	136.5	0.0	3.2

2000	0.0	0.0	9.0	114.3	36.4	71.0	106.6	397.9	106.6	107.1	62.5	36.0
2001	0.0	24.0	84.8	25.1	81.2	107.3	310.0	362.7	76.3	19.5	0.0	5.0
2002	15.2	6.8	78.7	4.3	106.6	41.9	252.8	200.2	34.5	0.0	0.0	5.4
2003	15.0	68.0	101.9	7.2	106.6	98.2	252.3	227.8	94.9	34.2	19.4	12.9
2004	7.8	6.3	23.4	63.0	7.6	46.0	252.3	286.8	71.6	92.7	106.6	12.4

APPENDIX : D Daily stream flow data of Suha Gaging station for some selected years

1986	Jan	Feb	Mar	Apr	May	Jun	Jul	Aug	Sep	Oct	Nov	Dec
1	0.9	0.9	0.5	0.8	0.5	0.5	0.3	6.7	40.2	10.1	2.9	1.5
2	0.8	0.5	0.7	0.5	0.5	0.3	6.0	33.7	8.0	4.1	1.3	0.9
3	0.8	0.5	0.6	0.6	0.5	0.3	5.0	17.1	7.1	13.5	1.3	0.9
4	0.8	0.4	0.6	0.6	0.5	0.3	4.1	24.6	4.4	4.8	1.2	0.9
5	0.7	0.4	0.6	0.6	0.5	0.3	3.4	33.7	3.3	3.7	1.2	0.9
6	0.7	0.4	0.6	0.6	0.5	0.3	3.5	28.9	4.7	3.3	1.2	0.9
7	0.7	0.5	0.6	0.6	0.5	0.3	3.6	18.0	14.1	2.9	1.1	0.8
8	0.7	0.5	0.6	0.6	0.5	0.4	3.4	18.2	10.1	2.6	1.1	0.8
9	0.7	0.6	0.6	0.5	0.5	0.4	3.8	24.5	10.7	2.4	1.1	0.8
10	0.7	0.7	0.6	0.5	0.5	0.4	7.9	38.7	26.2	2.3	1.1	0.8
11	0.7	0.8	0.6	0.5	0.6	0.4	8.3	43.0	36.1	2.1	1.1	0.8
12	0.7	0.9	0.6	0.4	0.6	0.4	8.5	41.4	22.0	2.0	1.1	0.8
13	0.7	0.8	0.7	0.4	0.6	0.4	8.0	15.3	9.6	1.8	1.1	0.8
14	0.7	0.8	0.7	0.4	0.6	0.5	5.5	13.5	5.7	1.8	1.0	0.8
15	0.7	0.8	0.8	0.4	0.6	1.0	4.8	12.0	4.1	1.7	1.0	0.7
16	0.7	0.8	0.7	0.5	0.6	1.2	3.5	15.6	7.3	1.7	1.0	0.7
17	0.7	0.8	0.7	0.6	0.6	1.2	9.9	13.9	5.3	1.6	1.0	0.6
18	0.7	0.8	0.7	0.6	0.6	1.3	6.4	14.3	3.5	1.6	1.0	0.6
19	0.7	0.7	0.7	0.6	0.6	1.3	7.8	13.9	3.5	1.5	1.0	0.6
20	0.7	0.6	0.6	0.6	0.5	1.5	6.3	13.5	9.5	1.4	1.0	0.6
21	0.7	0.6	0.6	0.6	0.5	1.6	5.6	13.7	17.0	1.4	1.0	0.6
22	0.7	0.6	0.6	0.6	0.5	1.8	4.2	13.3	10.1	1.5	1.0	0.6
23	0.7	0.6	0.6	0.6	0.5	1.8	2.5	12.0	5.8	1.8	1.0	0.6
24	0.6	0.6	0.6	0.6	0.5	1.8	23.8	6.7	3.2	2.1	1.0	0.6
25	0.6	0.6	0.6	0.7	0.4	2.1	20.9	19.8	2.0	2.0	1.0	0.6
26	0.6	0.8	0.6	0.6	0.4	3.0	16.5	34.6	1.3	1.8	1.0	0.6
27	0.6	0.9	0.5	0.6	0.4	3.5	14.7	24.1	2.5	1.7	1.0	0.6
28	0.6	0.8	0.5	0.5	0.3	6.5	14.6	10.4	3.5	1.6	1.0	0.9
29	0.6	0.0	0.5	0.5	0.3	5.9	18.6	37.6	2.6	1.5	0.9	0.9
30	0.6	0.0	0.6	0.5	0.3	5.9	39.9	15.3	2.3	1.4	0.9	0.9
31	0.5	0.0	0.6	0.0	0.3	0.0	19.6	19.3	0.0	1.4	0.0	0.9

1987	Jan	Feb	Mar	Apr	May	Jun	Jul	Aug	Sep	Oct	Nov	Dec
1	0.7	0.9	0.5	0.4	0.8	0.5	2.5	0.9	8.9	4.0	1.2	0.9
2	0.8	0.5	0.4	0.7	0.5	2.3	1.0	11.6	3.4	1.2	0.9	0.6
3	0.8	0.5	0.4	0.6	0.5	2.7	1.2	28.3	3.0	1.3	0.9	0.6
4	0.9	0.5	0.4	0.7	0.6	3.5	1.2	22.1	2.5	1.3	0.9	0.6
5	0.9	0.5	0.5	1.5	0.5	7.2	1.0	19.5	2.3	1.2	0.9	0.6
6	0.9	0.5	0.5	1.0	0.4	3.8	1.1	16.4	2.4	1.2	0.9	0.6
7	0.9	0.5	0.5	0.8	0.4	2.9	0.7	12.3	2.4	1.3	0.9	0.6
8	0.8	0.5	0.6	0.7	0.4	5.5	0.9	8.5	2.5	1.3	0.9	0.7
9	0.8	0.5	0.6	0.7	0.5	13.8	1.1	9.7	2.9	1.3	0.8	1.2
10	0.8	0.5	0.6	0.6	0.4	3.5	0.7	12.0	2.8	1.3	0.8	1.2
11	0.6	0.5	0.6	0.9	0.5	1.9	0.5	21.0	2.6	1.3	0.8	1.0
12	0.6	0.5	0.7	1.6	1.2	1.8	0.5	19.6	2.2	1.5	0.8	0.8
13	0.9	0.5	0.8	1.0	1.1	2.2	0.9	12.1	1.9	1.3	0.8	0.7
14	0.9	0.5	0.9	0.8	1.0	1.8	1.1	21.0	1.8	1.2	0.8	0.7
15	0.9	0.5	1.6	0.7	0.8	1.7	1.2	24.2	1.7	1.2	0.8	0.7
16	0.8	0.5	1.3	0.7	0.7	1.6	1.2	24.3	1.5	1.2	0.8	0.7
17	0.8	0.5	0.9	0.6	0.7	1.5	1.3	21.6	1.5	1.2	0.8	0.7
18	0.8	0.6	0.9	0.7	0.6	1.7	1.8	17.5	1.4	1.2	0.8	0.7
19	0.8	0.6	0.8	0.8	0.6	1.8	4.8	19.6	1.3	1.2	0.8	0.7
20	0.8	0.5	1.0	0.9	1.0	1.2	2.7	19.9	1.3	1.2	0.8	0.6
21	0.8	0.5	1.1	0.8	2.5	0.9	2.9	19.7	1.3	1.1	0.8	0.6
22	0.8	0.5	1.3	0.7	2.4	0.9	2.7	18.4	1.3	1.1	0.8	0.6
23	0.8	0.5	1.6	0.7	2.7	0.7	2.3	20.1	1.3	1.1	0.8	0.6
24	0.7	0.5	2.1	0.6	2.7	0.9	2.3	18.2	1.3	1.1	0.7	0.6
25	0.6	0.5	2.7	0.6	3.6	1.0	2.9	15.8	1.3	1.1	0.7	0.6
26	0.6	0.5	3.4	0.6	4.9	1.2	3.9	8.5	1.8	1.0	0.7	0.6
27	0.6	0.5	2.6	0.5	8.1	1.2	10.7	8.1	1.8	1.0	0.7	0.6
28	0.6	0.5	2.1	0.5	7.1	0.9	7.4	7.3	1.7	1.0	0.7	0.6
29	0.5	0.0	1.7	0.5	3.6	0.9	6.2	6.7	1.5	1.0	0.7	0.6
30	0.5	0.0	1.3	0.5	1.0	0.7	9.1	6.7	1.3	1.0	0.7	0.6
31	0.5	0.0	0.9	0.0	1.2	0.0	9.2	4.9	0.0	0.9	0.0	0.6

APPENDIX : E HEC HMS Outputs

APPENDIX : E1 Global Summary result for calibration run (1986-1998)

Global Summary Results for Run "Calibration Run"

Project: Suha Watershed Simulation Run: Calibration Run

Start of Run: 01Jan1986, 00:00
End of Run: 31Dec1998, 00:00
Compute Time: DATA CHANGED, RECOMPUTE

Basin Model: Basin_Calibration
Meteorologic Model: Met_Calibration
Control Specifications: Control_Calibration

Show Elements: All Elements | Volume Units: (•) MM ( ) 1000 M3 | Sorting: Hydrologic

Hydrologic Element	Drainage Area (KM2)	Peak Discharge (M3/S)	Time of Peak	Volume (MM)
S_1	52.570	2.8	13Aug1986, 00:00	2017.58
S_3	27.806	1.8	07Aug1986, 00:00	1982.51
J_5	80.376	3.8	12Aug1986, 00:00	2005.44
R_5	80.376	3.8	12Aug1986, 00:00	2005.45
S_2	154.000	4.1	22Aug1986, 00:00	1998.03
S_7	67.384	2.8	14Aug1986, 00:00	1998.91
J_4	301.760	8.8	14Aug1986, 00:00	2000.20
R_4	301.760	8.8	14Aug1986, 00:00	2000.20
S_4	31.541	2.5	06Aug1986, 00:00	1975.15
S_8	21.444	2.0	06Aug1986, 00:00	1989.56
J_3	354.745	10.3	12Aug1986, 00:00	1997.33
R_3	354.745	10.3	12Aug1986, 00:00	1997.33
S_9	65.061	3.8	08Aug1986, 00:00	1992.40
S_5	27.738	2.3	06Aug1986, 00:00	1974.57
J_2	447.544	14.0	12Aug1986, 00:00	1995.20
R_2	447.544	14.0	12Aug1986, 00:00	1995.20
S_6	32.613	5.5	05Aug1986, 00:00	2015.07
S_10	21.639	3.2	05Aug1986, 00:00	2015.07
J_1	501.796	17.6	05Aug1986, 00:00	1997.35
S_11	287.990	17.3	09Aug1986, 00:00	2015.04
R_1	501.796	17.5	05Aug1986, 00:00	1997.37
Suha outlet	664.8	32.8	11Aug1986, 00:00	2003.81

APPENDIX : E2 Global Summary result for validation run (1999-2004)

Global Summary Results for Run "Validation Run"

Project: Suha Watershed Simulation Run: Validation Run

Start of Run: 01Jan1999, 00:00
End of Run: 31Dec2004, 00:00
Compute Time:DATA CHANGED, RECOMPUTE

Basin Model: Basin_Validation
Meteorologic Model: Met_Validation
Control Specifications:Control_ Validation

Show Elements: All Elements Volume Units: MM 1000 M3 Sorting: Hydrologic

Hydrologic Element	Drainage Area (KM2)	Peak Discharge (M3/S)	Time of Peak	Volume (MM)
S_1	52.570	2.7	19Jul2001, 00:00	1070.46
S_3	27.806	1.8	15Jul2001, 00:00	1043.36
J_5	80.376	4.1	16Jul2001, 00:00	1061.08
R_5	80.376	4.1	16Jul2001, 00:00	1061.08
S_2	154.000	5.6	04Aug2001, 00:00	1052.38
S_7	67.384	3.3	20Jul2001, 00:00	1058.86
J_4	301.760	11.0	26Jul2001, 00:00	1056.14
R_4	301.760	11.0	26Jul2001, 00:00	1056.13
S_4	31.541	2.1	14Jul2001, 00:00	1040.27
S_8	21.444	1.5	15Jul2004, 00:00	1049.88
J_3	354.745	13.5	25Jul2001, 00:00	1054.35
R_3	354.745	13.5	25Jul2001, 00:00	1054.34
S_9	65.061	4.3	14Jul2001, 00:00	1060.15
S_5	27.738	2.0	15Jul2004, 00:00	1042.14
J_2	447.544	18.6	15Jul2001, 00:00	1054.43
R_2	447.544	18.6	15Jul2001, 00:00	1054.42
S_6	32.613	3.3	14Jul2004, 00:00	1082.91
S_10	21.639	1.8	15Jul2004, 00:00	1083.55
J_1	501.796	21.9	14Jul2001, 00:00	1057.53
S_11	287.990	19.1	15Jul2001, 00:00	1084.13
R_1	501.796	21.9	14Jul2001, 00:00	1057.52
Suha outlet	664.8	40.9	14Jul2001, 00:00	1067.22

APPENDIX : E3 Flood magnitude at different return period

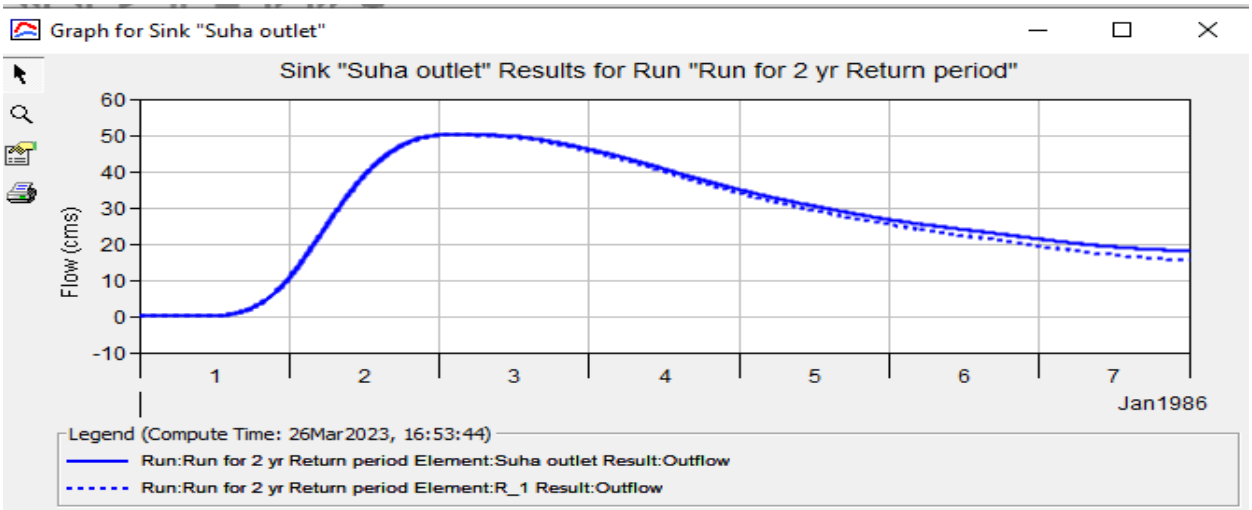

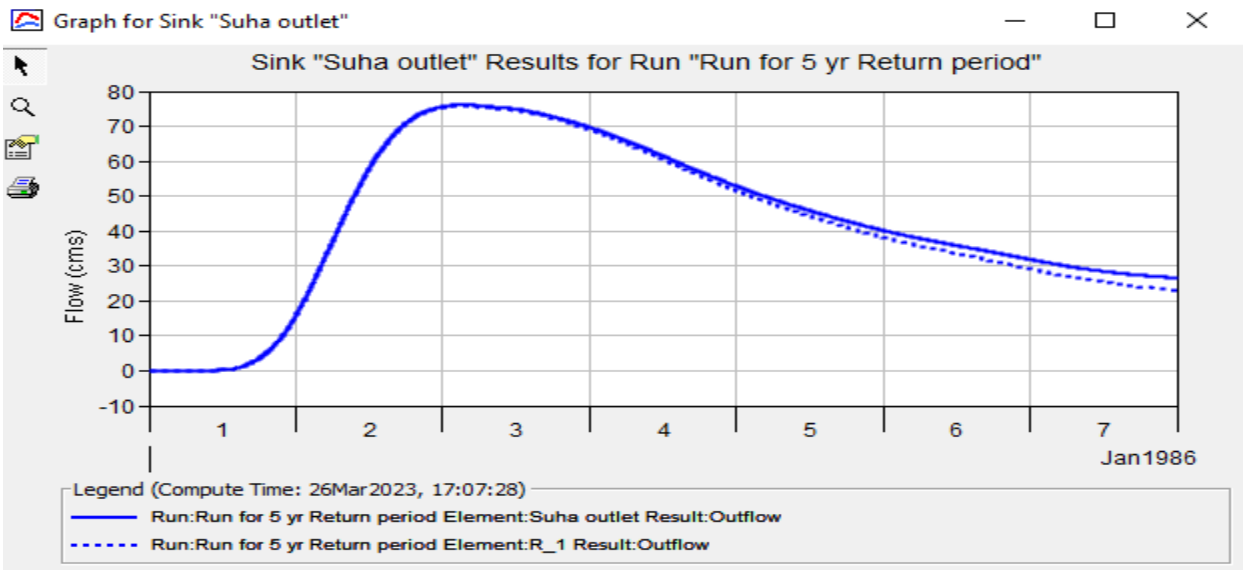
Graph for Sink "Suha outlet"
Sink "Suha outlet" Results for Run "Run for 5 yr Return period"
Flow (cms)
80
70
60
50
40
30
20
10
0
-10
1
2
3
4
5
6
7
Jan1986
Legend (Compute Time: 26Mar2023, 17:07:28)
Run:Run for 5 yr Return period Element:Suha outlet Result:Outflow
Run:Run for 5 yr Return period Element:R_1 Result:Outflow

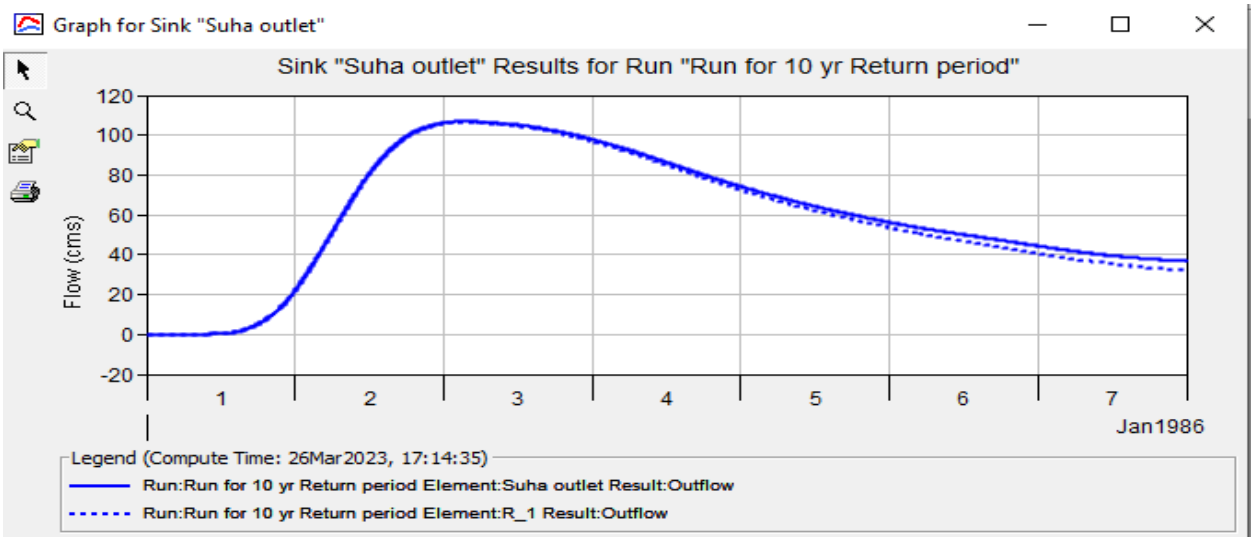
Graph for Sink "Suha outlet"
Sink "Suha outlet" Results for Run "Run for 10 yr Return period"
Flow (cms)
120
100
80
60
40
20
0
-20
1
2
3
4
5
6
7
Jan1986
Legend (Compute Time: 26Mar2023, 17:14:35)
Run:Run for 10 yr Return period Element:Suha outlet Result:Outflow
Run:Run for 10 yr Return period Element:R_1 Result:Outflow

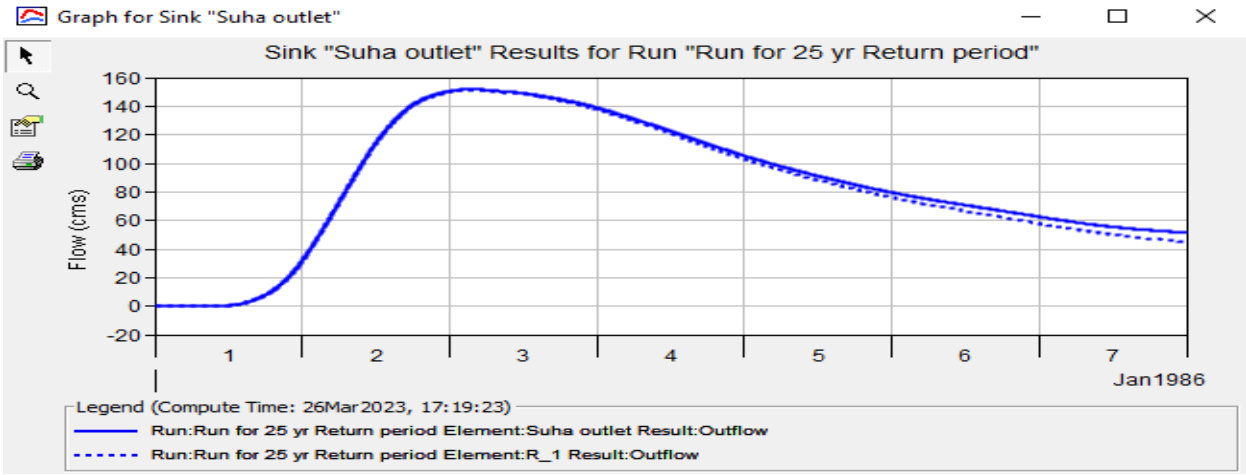
Graph for Sink "Suha outlet"
Sink "Suha outlet" Results for Run "Run for 25 yr Return period"
Flow (cms)
160
140
120
100
80
60
40
20
0
-20
1
2
3
4
5
6
7
Jan1986
Legend (Compute Time: 26Mar2023, 17:19:23)
Run:Run for 25 yr Return period Element:Suha outlet Result:Outflow
Run:Run for 25 yr Return period Element:R_1 Result:Outflow

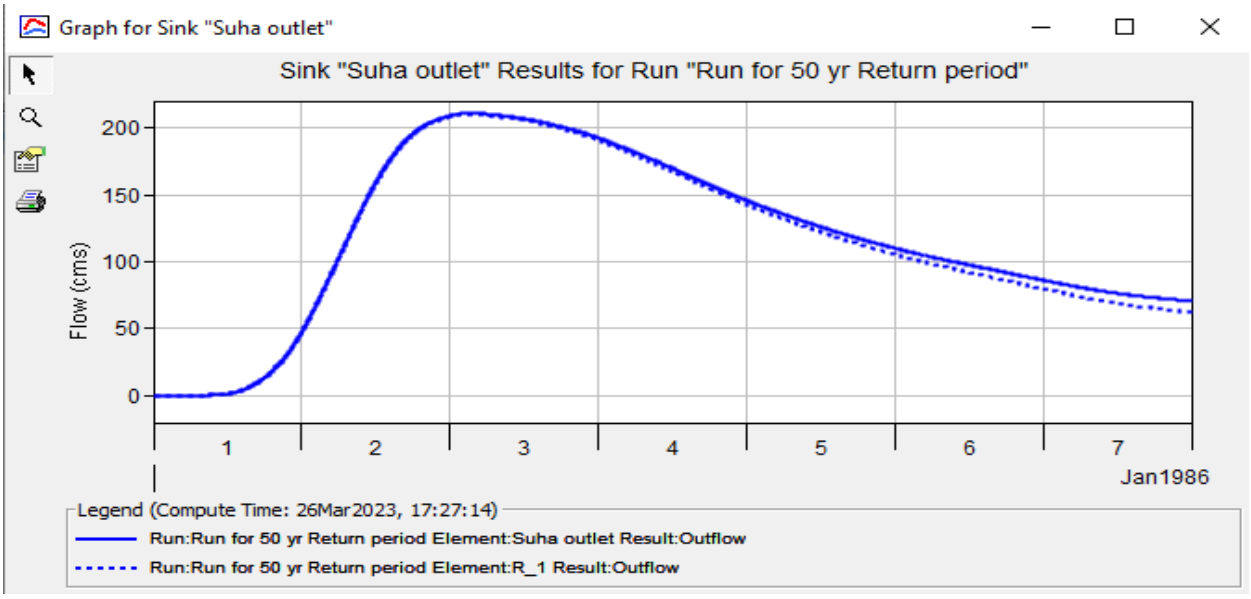
Graph for Sink "Suha outlet"
Sink "Suha outlet" Results for Run "Run for 50 yr Return period"
Flow (cms)
200
150
100
50
0
1
2
3
4
5
6
7
Jan1986
Legend (Compute Time: 26Mar2023, 17:27:14)
Run:Run for 50 yr Return period Element:Suha outlet Result:Outflow
Run:Run for 50 yr Return period Element:R_1 Result:Outflow

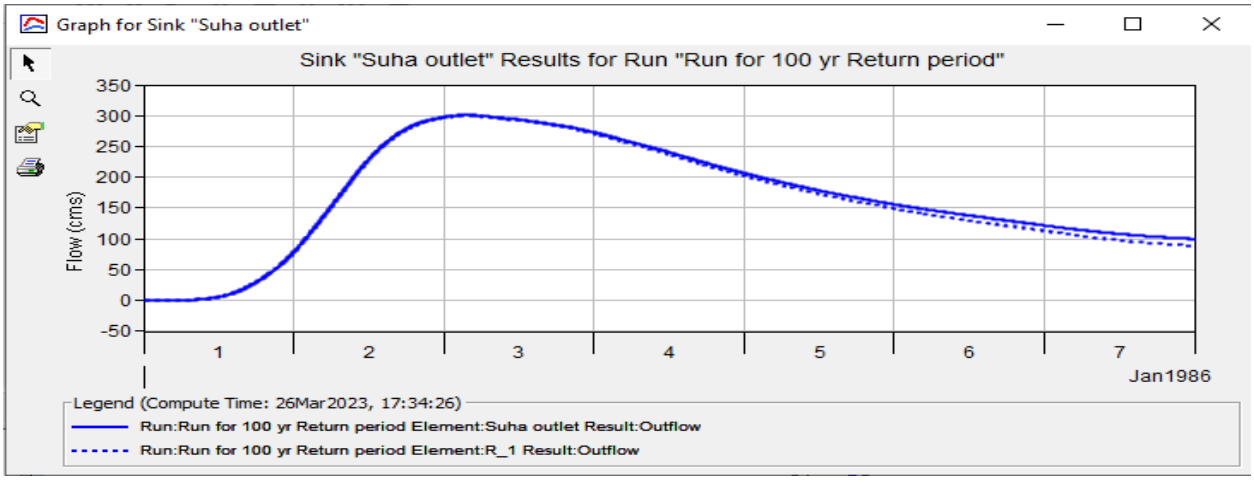
Graph for Sink "Suha outlet"
Sink "Suha outlet" Results for Run "Run for 100 yr Return period"
Flow (cms)
350
300
250
200
150
100
50
0
-50
1
2
3
4
5
6
7
Jan1986
Legend (Compute Time: 26Mar2023, 17:34:26)
Run:Run for 100 yr Return period Element:Suha outlet Result:Outflow
Run:Run for 100 yr Return period Element:R_1 Result:Outflow